Royal College of Surgeons in Ireland

repository@rcsi.com

Lipid Raft association restricts CD44-ezrin interaction and promotion of breast cancer cell migration.

AUTHOR(S)

Simona Donatello, Irina S. Babina, Lee D. Hazelwood, Arnold DK Hill, Ivan R. Nabi, Ann M. Hopkins

CITATION

Donatello, Simona; Babina, Irina S.; Hazelwood, Lee D.; Hill, Arnold DK; Nabi, Ivan R.; Hopkins, Ann M. (2012): Lipid Raft association restricts CD44-ezrin interaction and promotion of breast cancer cell migration.. Royal College of Surgeons in Ireland. Journal contribution. https://hdl.handle.net/10779/rcsi.10800425.v1

HANDLE

10779/rcsi.10800425.v1

LICENCE

CC BY-NC-ND 4.0

This work is made available under the above open licence by RCSI and has been printed from https://repository.rcsi.com. For more information please contact repository@rcsi.com

URL

https://repository.rcsi.com/articles/journal_contribution/Lipid_Raft_association_restricts_CD44-ezrin_interaction_and_promotion_of_breast_cancer_cell_migration_/10800425/1

LIPID RAFT ASSOCIATION RESTRICTS CD44-EZRIN INTERACTION AND PROMOTION OF BREAST CANCER CELL MIGRATION

Simona Donatello[1§], Irina S. Babina[1§], Lee D. Hazelwood[2], Arnold D.K. Hill[1], Ivan R. Nabi[3], Ann M. Hopkins[1]*

[1]Department of Surgery, Royal College of Surgeons in Ireland, Dublin, Ireland,

[2]University of Leeds; Leeds, UK,

[3] Department of Cellular and Physiological Sciences, Life Sciences Institute, University of British Columbia, Vancouver, BC, Canada.

Number of text pages: 36, **number of tables:** 0, **number of figures:** 9.

Short running head: Lipid rafts and breast cancer cell migration

Grant number and sources of support:

Cancer Research Ireland (CRI05HOP/AMH), The Irish Research Council for Science, Engineering & Technology (EMBARK 2005/SD), Health Research Board of Ireland (HRA/2009/49 to AMH), Breast Cancer Ireland, EU-funded Network of Excellence ENFIN (LSHG-CT-2005-518254) and the UK Medical Research Council (LDH). The confocal microscope and ultracentrifuge were funded through the National Biophotonics and Imaging Platform, Ireland, and funded by the Irish Government's Programme for Research in Third Level Institutions, Cycle 4, Ireland's EU Structural Funds Programmes 2007 - 2013.

***Address correspondence to:** Ann M. Hopkins, Dept. of Surgery, Royal College of Surgeons in Ireland, RCSI Education and Research Centre, Beaumont Hospital, Dublin 9, IRELAND.

Tel: +353-1-809-3858; Fax: +353-1-633-5082, Email: annhopkins@rcsi.ie

[§] These authors contributed equally to this study.

ABSTRACT

Cancer cell migration is a key early step in metastasis, the main cause of breast cancer-related deaths. Cholesterol-enriched membrane domains known as lipid rafts influence the function of many cellular proteins including the raft-associated protein CD44. We describe a novel mechanism whereby lipid rafts regulate the interaction between CD44 and its binding partner ezrin in migrating breast cancer cells. Specifically, in non-migrating cells CD44 and ezrin localized to different membranous compartments; CD44 being predominantly affiliated with lipid rafts and ezrin with non-raft compartments. After the induction of migration (either non-specific or CD44-driven), the association of CD44 with lipid rafts was decreased. This was accompanied by increased co-precipitation of CD44 and active (threonine-phosphorylated) ezrin-radixin-moesin (ERM) proteins in non-raft compartments and increased co-localization of CD44 with the non-raft protein, transferrin receptor. Pharmacological disruption of lipid rafts using methyl-β-cyclodextrin also increased CD44/ezrin co-precipitation and co-localization, further suggesting CD44 interacts with ezrin outside lipid rafts during cell migration. Conversely, promoting CD44 retention inside lipid rafts by pharmacological inhibition of depalmitoylation virtually abolished CD44/ezrin interactions. However, transient knockdown of either flotillin-1 or caveolin-1 or their double knockdown was not sufficient to increase cell migration over a short timecourse; suggesting complex crosstalk mechanisms. We propose a new model for CD44-dependent breast cancer cell migration, where CD44 must re-localize outside lipid rafts to drive cell migration. This could have implications for rafts as pharmacological targets to down-regulate cancer cell migration.

INTRODUCTION

The membrane protein CD44 is a multi-faceted molecule involved in many different cellular processes including organ development, neuronal axon guidance, immune functions, haematopoiesis and migration [1-4]. It acts as a receptor for the extracellular matrix (ECM) component hyaluronic acid (HA) [5, 6] and for the secreted extracellular protein osteopontin [7]. CD44 is an important mediator of cellular adhesion and migration due to its active influence on the organization of the actin cytoskeleton. This occurs through direct interactions between CD44 and different actin-binding partners; of which the most common are proteins belonging to the ERM (ezrin, moesin, radixin) family. The ERM proteins form a bridge between CD44 and the actin cytoskeleton, mediating cell morphology changes that are important for cell migration. Ezrin interacts with CD44 and F-actin respectively through its conserved N-terminal FERM domain (band-Four point one, Ezrin, Radixin, Moesin) and C-terminal CERMAD domain (C-terminal ERM Association Domain). In the inactive configuration of ezrin, the FERM and CERMAD domains interact with each other and block the binding sites for CD44 and F-actin. Ezrin activation is mediated by phosphorylation-induced conformational changes [8], with phosphorylation on threonine-567 being necessary for binding to the F-actin cytoskeleton [9].

Phosphorylation of CD44 has also been shown to be important for its activation, particularly on serine residues in the C-terminal domain [8, 10]. CD44 has been described to be enriched in cholesterol- and sphingomyelin-enriched membrane microdomains termed lipid rafts [11]. Much evidence has suggested the involvement of lipid rafts in regulating different cellular events including migration [12]. Since some of these cellular events are frequently altered in cancer, it has been hypothesized that lipid rafts play a crucial role in regulating cancer progression [13]. However, although alterations in CD44 expression have been associated with many cancers [14], how lipid rafts influence the subcellular localization (and thus migratory functions) of CD44 and its contribution towards cancer progression is not well understood.

Whether or not CD44 and its binding partners localize to lipid rafts may in fact regulate several signaling cascades. CD44 is usually directed towards lipid rafts via post-translational lipid modifications called acylation reactions, the most common of which is palmitoylation. Due to its dynamic and reversible nature, palmitoylation can have important functions in dictating protein fate such as protein trafficking, lateral segregation and cellular localization. Palmitoylation plays an important role in CD44-HA turnover, with palmitoylated CD44 promoting CD44-HA endocytosis. Accordingly, lipid rafts have been described to play an important role in cellular endocytosis [15].

Ezrin localization to lipid rafts is controversial [16] and the mechanisms regulating its affiliation with lipid rafts incompletely understood. Ezrin interactions with phosphatidylinositol 4,5-biphosphate (PIP2) may be important for its activation, causing the FERM and CERMAD domains to open [17] and permitting ezrin localization at the plasma membrane [18]. Since PIP2 has been described to be enriched in lipid rafts [19], it is possible that ezrin localizes to lipid rafts through an interaction with PIP2.

In this paper, we set out to investigate the role of lipid rafts in regulating CD44-dependent breast cancer cell migration. Our initial findings revealed that CD44 and ezrin localized to different membrane fractions in non-migrating cells, biochemically characterized as lipid raft and non-raft domains respectively. In response to migratory stimuli (either random or CD44-specific), the proportion of raft-affiliated CD44 decreased while that of ezrin did not change. Moreover, under migrating compared to non-migrating conditions, immunofluorescence confocal microscopy revealed increased co-localization of CD44 with the non-raft marker transferrin receptor. Altogether w~~W~~e present novel evidence that physical interactions between CD44 and ezrin occur in non-raft fractions of migrating cells. In support of this, pharmacological disruption of lipid rafts increased CD44/ezrin co-precipitation, while enhanced retention of CD44 within rafts abolished CD44/ezrin co-precipitation. Surprisingly, flotillin-1 or caveolin-1 transient knockdown alone did not affect cell migration in these cells; suggesting compensatory mechanisms which make up for the presumed loss of one or other raft compartment. In support of this assumption, coincident knockdown of flotillin-1 and caveolin-1 significantly impaired cell migration. Nonetheless, our data are consistent with a novel

regulatory mechanism in which CD44 translocates outside lipid rafts to bind ERM binding partners such as ezrin and drive cell migration. Future exploration of the precise mechanisms regulating this translocation may reveal future targets for interfering with breast cancer cell migration during the early stages of metastasis.

MATERIALS AND METHODS

Antibodies and reagents. CD44 antibodies were purchased from Santa Cruz (immunoprecipitations and immunofluorescence), Abcam and R&D Systems (Western blotting); ezrin from BD Biosciences; phospho-threonine-ERM from Cell Signalling Technologies, flotillin-1 from BD Biosciences, actin from Sigma-Aldrich, caveolin-1 from Cell Signaling Technologies, radixin and moesin from GeneTex/Source Biosciences, transferrin receptor and Alexa-Fluor secondary antibodies from Invitrogen. Triton X-100 (10%) was purchased from Roche; protein G-sepharose 4B from GE Healthcare.

Cell culture. MDA-MB-231 cells were obtained from the ATCC and cultured in DMEM, 10% fetal bovine serum, 2mM L-glutamine, 100U/ml penicillin and 100µg/ml streptomycin. MDA-MB-231 cells stably knocked-down for caveolin-1 via a vector containing shRNA against caveolin-1 and carrying a resistance cassette for blastocidine (Invitrogen)[20] were cultured similarly but with the addition of 5ng/µl blasticidine. For some experiments, siRNA against flotillin-1 or caveolin-1 was used to transiently knockdown gene expression for 72h before performing migration assays or immunofluorescence analysis. In brief, cells were grown at low density for up to 24h on 24-well plates or 13mm coverslips and transfected with 25nM siRNA against flotillin-1 or caveolin-1 (Dharmafect SmartPools) or a universal negative control siRNA (Dharmafect) using Dharmafect-1 reagent as per manufacturer's instructions (Dharmacon).

Cell treatments. Methyl-β-cyclodextrin (MβCD, 10mM, Sigma) was used to disrupt lipid raft physiology by cholesterol depletion as already described [21-23]. MβCD was prepared in serum-free medium and added to confluent 10cm dishes of cells for 30 minutes prior to wounding with a sterile pipette tip attached to a vacuum. In order to convert a proportion of cells into spreading and migrating

cells, monolayers were extensively wounded by making 9 horizontal and 9 vertical scratches per dish using a sterile pipette tip attached to suction. Depalmitoylation inhibitors (DPI) Methyl Arachidonyl Fluorophosphonate (MAFP, 5µM) and Palmityl Trifluoromethyl Ketone (PTK, 20µM) were obtained from Cayman Chemicals and incubated with cells for 30 minutes prior to wounding. All treated cells were washed once and allowed to migrate in serum-free medium for the indicated times. Confluent cells were wounded and treated for 30 minutes with 5mg/ml HA where indicated.

Scratch-wound migration assays. Cells were grown to confluence in 24-well plates and scratch-wounded once using a sterile pipette tip attached to a vacuum. Cells were then washed once and incubated in the relevant treatments in serum-free medium. Wounds were photographed at specific time points on a phase contrast microscope linked to a charge-coupled device camera (Olympus), and the wound size at a single reference point measured over time using Cell B software (Olympus).

Immunofluorescence microscopy. Cells were grown to confluence on sterile coverslips, treated as indicated and fixed in 3.7% paraformaldehyde (pH 7.4) for 10 minutes at room temperature, in ice-cold ethanol for 20 minutes at -20ºC or in ice-cold 80% methanol/20% acetone. Primary antibody and secondary antibodies (diluted in 5% normal goat serum) were incubated for 1 hour at room temperature. Nuclei were counterstained with DAPI for 10 minutes at room temperature. Each step was followed by three washes in phosphate-buffered saline (PBS). Coverslips were mounted in PBS:glycerol:*p*-phenylenenediamine hydrochloride (1:1:0.01 v/v/v) and visualized on a Zeiss LSM 510-meta or 710-meta confocal microscope using 63x oil immersion lenses.

Protein immunoprecipitations. Cells were washed in cold PBS, lysed and scraped in Relax buffer (100mM KCl, 3mM NaCl, 3.5mM $MgCl_2$, 10mM HEPES) containing 1% Triton X-100 and protease and phosphatase inhibitor cocktails (Sigma-Aldrich). Lysates were dounced 20 times and centrifuged at 1500g at 4°C for 5 minutes. Equivalent amounts of total protein per treatment condition (eg. migrating versus non-migrating cell lysates) were used in matched immunoprecipitation experiments. After a pre-clear step with Protein G-sepharose, 3µg of mouse anti-human CD44 antibody (or an equivalent concentration of control mouse IgG) was added to each sample and rotated overnight at 4°C. Immunocomplexes were collected by rotation with 50µl of protein G-sepharose for 3 hours at

4°C. Immunocomplexes were washed three times with lysis buffer, resuspended in 2X Laemelli reducing sample buffer, boiled and analyzed by SDS-PAGE and Western blotting.

Lipid raft isolation. Two confluent 10cm dishes per condition were treated as described. Hanks balanced salt solution (HBSS) containing calcium, magnesium and 10mM HEPES (Sigma) was used to wash cells before scraping them into 400µL/dish lysis buffer (HBSS, 1% Triton-X100, protease and phosphatase inhibitors). Lysates were dounced 20x and triturated 20x through a 26-gauge needle. At 4°C, lysates were mixed 1:1 with a 90% (w/v) sucrose solution (in HBSS) and loaded at the bottom of a micro-ultracentrifuge tube. This was then overlain sequentially with solutions of 30%, 20% and 5% sucrose (w/v) and ultracentrifuged in an RP55S rotor at 281,591g for 19h at 4ºC in a Sorvall RC M120EX microultracentrifuge.

.Starting from the top of the tube (fractions of lowest sucrose density), gradients were fractionated manually at 4°C into six equal-volume fractions. For some experiments, continuous sucrose gradients were prepared from 2 x 10cm dishes of confluent cells in larger (12ml) tubes essentially as described [24, 25]. Briefly, cell lysates were prepared in 2.5 ml HBSS containing 1% Triton X-100 and a protease inhibitor cocktail. At 4ºC, 2ml of lysate was mixed with 2 ml of 60% sucrose and placed at the bottom of an ultracentrifuge tube. A 200 µl "cushion" of 30% sucrose was manually layered on top, whereupon a continuous 30-5% gradient was poured using an Auto-Densi Flow density gradient fractionator (Labconco). Gradients were ultracentrifuged at 39,000 rpm /19h / 4ºC in a Beckman Optima L-100K ultracentrifuge (Sw41 rotor) and fractionated manually into 12 x 1ml fractions. In each case, a peak of alkaline phosphatase activity and enriched flotillin-1 expression was used to identify lipid raft fractions. Since both peaked at ~20-26% sucrose irrespective of the gradient preparation, the small and large gradient preparations were highly comparable even though fraction numbers did not directly correlate. For clarity in Western blot results, sucrose densities of gradient fractions have been presented instead of fraction numbers; and fractions with peak alkaline phosphatase activity have been highlighted with circles.

SDS-PAGE and Western blot analysis. Since protein concentrations were non-uniform across gradient fractions, 5µg of protein per lane (unless otherwise indicated) was separated on fixed-percentage acrylamide gels at 40mA constant current. To control for the possibility that equivalent protein loading

would induce artifacts not present under equivalent volume loading conditions, electrophoresis of equivalent fraction volumes was also performed in representative blots and confirmed to have a similar outcome (**Supplementary Figure S1)**. Proteins were then transferred to nitrocellulose membranes at a constant voltage of 100V for 1h and blocked in 5% non-fat dry milk Tris-buffered saline (TBS)-0.1% Tween for 1h at RT. Primary (as indicated) and secondary (mouse-, rabbit- or rat-HRP conjugated, Sigma) antibodies were prepared in 5% non-fat dry milk in TBS containing 0.1% Tween-20 (TBS-T). Primary antibodies were incubated overnight at 4°C, and secondary antibodies for 1h at room temperature. Each step was followed by 3x 10 minute washes in TBS-T. Luminescent signals were developed onto Kodak film after incubation with Western Lightning enhanced chemiluminescent reagent (Perkin Elmer).

Image analysis .Densitometric analysis of Western blot films was performed using Image J software (National Institutes of Health). Pixel co-localization of different colour channels in confocal images was analyzed by Image J software using the plugins "ColocalizeRGB" and "Area calculator".

Migration matrix and pathway reconstruction. Immunoprecipitation changes observed within migrating cells relative to non-migrating cells were used to infer the signalling network using logical reasoning [26]. For example, movement of CD44 from lipid raft to non-raft regions was presumed if a decrease of CD44 in raft fractions accompanied by an increase of CD44 in non-raft fractions was observed. Other network paths were constructed in the same manner with the additional model constraint and assumption that CD44 only binds to ezrin in its phosphorylated state[8]. In all cases, there was an explicit assumption that the total amount of CD44, ezrin and phospho-ERM remained constant within cells over the timecourse of individual experiments (confirmed in **Supplementary Fig. S2**).

Statistical analysis. Data were expressed as mean ± standard error of the mean. Different conditions were compared using unpaired Student's *t*-tests and non-parametric tests. Linear regression analysis in GraphPad Prism v5 was used to test statistical differences between the slopes of scratch wound assays under different treatment conditions.

RESULTS

CD44 and ezrin interact at the migrating edge in MDA-MB-231 cells.

Although the involvement of CD44 in breast cancer migration has been described in many settings, the regulatory mechanisms are incompletely understood and often conflicting. A likely mechanism is that CD44 interacts with the actin cytoskeleton through ezrin, a member of the ERM family [27]. We used scratch-wounding as a tool to induce migration in MDA-MB-231 breast cancer cells in order to study the role of lipid rafts in regulating CD44 and ezrin interactions. Monolayers of cells were extensively wounded by making 9 horizontal and 9 vertical scratches per 10cm dish. The total number of migrating cells per experiment was estimated by surface area calculations to be less than 10%. Since the mechanical stress applied by scratch wounding directly stimulates migration 3 to 5 cell diameters back from the wound edge[28], the depth covered by 3 to 5 cells along each side of each wound was used to calculate the estimated total migrating surface. However, it is well known that migrating cells secrete factors that can affect signaling even in cells distal to those that are directly migrating[29]. Since CD44/ezrin interactions are reportedly rapid and transient [8], MDA-MB-231 cells were allowed to migrate for 30 minutes in serum-free medium following scratch wounding. CD44 immunoprecipitate complexes were separated by SDS-PAGE and analyzed by immunoblotting for the presence of ezrin and CD44. **Figure 1A** shows that CD44 recovery was marginally increased in migrating cells (M) compared to non-migrating (NM) cells. However, a substantial increase in ezrin recovery was observed in CD44 immunoprecipitates of migrating cells compared to non-migrating controls, even though CD44 and actin levels in the input lysates were confirmed to be similar between treatment conditions (right inset). Furthermore, expression levels of CD44 and ezrin were observed to be stable over a migration timecourse from 30 minutes to 4 hours (**Supplementary Figure S2**).

In order to interact with CD44 and the cytoskeleton, ezrin must undergo post-translational conformational changes induced by phosphorylation on threonine-567. We used an antibody that recognises the phosphorylation of threonine-567 on ezrin and also the corresponding phospho-sites on moesin and radixin, related proteins belonging to the ERM family. Like ezrin, radixin and moesin are also highly expressed in MDA-MB-231 cells and exhibit stable levels over a migration timecourse (**Supplementary Figure S2**). As shown in **Figure 1A**, threonine-phosphorylated levels of the ERM

proteins (p-ERM) were slightly increased in migrating cells compared to non-migrating controls, but with little overall change in the ratio of p-ERM to total ezrin under migrating versus non-migrating conditions. Neither CD44 nor ezrin were detected in lysates immunoprecipitated with a non-specific control IgG antibody.

Co-localization of CD44 and ezrin under migrating (M) and non-migrating (NM) conditions was also examined by confocal immunofluorescence microscopy (**Figure 1B**). In migrating cells, the merged image of CD44 (green) and ezrin (red) demonstrated significantly increased co-localization particularly at the migrating edge (**Figure 1B**, **graph and inset,** differences in pixel overlap $p<0.05$). This suggested that changes in CD44 and ezrin localization within specific cellular regions accompanied cell migration. Localization of p-ERM relative to CD44 was also analyzed by confocal microscopy (**Figure 1C**). p-ERM specifically localized to membrane ruffles as already described [16, 30], and was highly polarized at the leading edge of migrating cells. p-ERM was the only protein examined which we observed to directly localize in filopodia-like structures at the edge of migrating cells (**Figure 1C, arrowheads**). At 30 minutes after induction of migration, CD44 and p-ERM localization was strongly identified anterior to such filipodia-like structures (**Figure 1C**). However no significant alteration in CD44/p-ERM co-localization by Image J analysis was detected (**Figure 1C**, graph, white bars). Interestingly CD44 expression in single planes measured appeared to decrease while that of p-ERM increased over time (**Figure 1C, graphs,** grey and black bars respectively).

CD44 and ezrin stably interact in non-lipid raft regions of migrating cells.

With evidence that CD44 and ezrin colocalize at the plasma membrane of migrating MDA-MB-231 cells, we next investigated whether they localized to the same biochemical compartments within membranes. Since CD44 has been described to localize to lipid raft domains, we first investigated the distribution of CD44 and ezrin relative to lipid raft membrane compartments. Lipid rafts were isolated from migrating or non-migrating MDA-MB-231 cells using non-detergent (data not shown) or detergent extraction methods in combination with isopycnic sucrose density gradient fractionation. Both methods yielded similar results. Gradient fractions were analyzed for enzyme activity of the lipid

raft marker alkaline phosphatase [31], protein concentration and sucrose density as shown in the representative graphs in **Figure 2A**. Top fractions from both small and large gradient preparations were characterized by low alkaline phosphatase activity, a sucrose density of <20%, and negligible protein content (**Figure 2A**). The exceptionally low protein content of these fractions mostly precluded their inclusion in SDS-PAGE gels. Conversely, middle fractions exhibited high alkaline phosphatase activity, a sucrose density of 20-25%, a low but measurable protein concentration and high expression of the lipid raft marker protein flotillin-1 (**Figure 2A-B**). Taken together, this was consistent with the enrichment of lipid rafts in these fractions. In contrast, the bulk of total cellular protein content was enriched in flotillin-low fractions at the bottom of sucrose gradients (sucrose density ≥30%). CD44 was observed to localize mainly in flotillin-enriched lipid raft fractions (**Figure 2B**), although it was not exclusively restricted to raft fractions. In contrast, ezrin was detected throughout flotillin-low fractions in a pattern similar to that of the non-raft protein actin (**Figure 2B**). Interestingly, the relative recovery of CD44 in flotillin-low (non-raft) fractions was increased after the induction of migration. This was further supported by a significant increase in CD44 co-localization with transferrin receptor, a known marker for non-raft domains, at the leading edge of migrating cells (**Supplementary Figure S3**). Quantification of the relative levels of CD44 in raft fractions (normalised to flotillin-1) versus non-raft fractions (normalised to ezrin) from multiple experiments confirmed a significant decrease in the quantity of raft-affiliated CD44 (**Figure 2B**, graph, $p<0.05$). Similar results were also obtained using the invasive breast cell line Hs578T (**Supplementary Figure S4~~3~~**).

We next used a co-immunoprecipitation approach to examine whether CD44/ezrin interactions took place inside or outside of lipid raft domains. Equal concentrations of total cellular protein from lipid raft and non-raft fractions of migrating (M) or non-migrating (NM) cells were immunoprecipitated with CD44 and analyzed for the presence of ezrin and p- ERM (**Figure 2C**). As expected, CD44 was highly enriched in lipid raft fractions of both migrating and non-migrating cells. However, CD44 recovery from lipid rafts in migrating cells was less than that in non-migrating cells; in conjunction with the appearance of a small pool of CD44 in immunoprecipitates from non-raft fractions of

migrating cells. Interestingly, ezrin was significantly enriched in CD44 immunoprecipitates recovered from non-raft fractions of migrating cells (**Figure 2C**). The absence of detectable ezrin bands in the other immunoprecipitate lanes does not exclude CD44/ezrin co-precipitation, but rather illustrates that such interactions take place at exceptionally low levels relative to the co-precipitation of CD44/ezrin in non-raft fractions from migrating cells. Interestingly, this suggests that even a very small pool of CD44 in non-raft fractions of migrating cells is sufficient to accounts for the bulk of interactions with ezrin. More importantly it also suggests that CD44 and ezrin interact outside lipid rafts during cell migration. Accordingly, p-~~Threonine-~~ERM showed a dramatic enrichment in non-raft fractions from CD44 immunoprecipitates of migrating cells (**Figure 2C**). These results further supported the hypothesis that interactions between CD44 and ERM proteins such as ezrin occur outside lipid rafts in migrating cells. However, since radixin and moesin are also expressed in MDA-MB-231 cells (**Supplementary Figure S2**), it is likely that the p-ERM signal reflects the combined presence of the activated form of each ERM family member, but in proportions that are as yet unknown. To begin interrogating the influence of lipid rafts on potential interactions between CD44 and radixin or moesin, a siRNA approach was used. Flotillin-1 or caveolin-1 (the two main structural proteins in lipid rafts) were separately knocked down in MDA-MB-231 cells, whereupon we checked for co-localization between CD44 and either moesin (**Figure 2D, top panel and Supplementary Figure S5**) or radixin (**Figure 2D, bottom panel and Supplementary Figure S5**). Interestingly flotillin-1 knockdown significantly decreased CD44 and moesin co-localization under non-migrating conditions relative to a siRNA negative control. Conversely, flotillin-1 knockdown significantly increased CD44 and radixin colocalization under non-migrating conditions compared to a siRNA negative control. This further supports that both moesin and radixin could contribute to the pERM signal co-precipitating with CD44 under non-migrating conditions (**Figure 2C**). It is also interesting to note that only flotillin-1 loss significantly affected the colocalization of CD44 with either moesin or radixin, suggesting a lack of involvement of caveolin-positive rafts in the process. However, decreased co-localization of CD44 with moesin was accompanied by decreased expression of the latter in flotillin-1 knockdown cells **(Supplementary Figure S5)**.

CD44 and ezrin binding is sensitive to raft disruption or altered CD44 raft affiliation.

To further probe the proposed interaction of CD44 and ezrin outside lipid raft domains in migrating MDA-MB-231 breast cancer cells, we tested the effect of pharmacological disruption of lipid rafts on CD44 / ezrin interactions. Confluent cells were treated with the cholesterol-sequestering reagent MβCD (10mM) in order to disrupt lipid rafts, then allowed to migrate in serum-free medium and immunoprecipitated for CD44. CD44 recovery was marginally increased in MβCD-treated cells compared to controls. However there was a large increase in ezrin recovery in CD44 immunoprecipitates from raft-disrupted (MβCD-treated) cells (**Figure 3A**). Western blotting quantification analysis revealed the increase in ezrin binding to CD44 MβCD-treated cells vs controls was statistically significant (**Figure 3A**, **graph**, p=0.0412). No significant alteration in p-ERM/CD44 co-precipitation was observed between control and MβCD-treated cells when each was normalised to their respective levels of total ezrin detected in CD44 immunoprecipitates (**Figure 3A** graph). Furthermore CD44 levels in the input lysates were confirmed to be similar between treatment conditions (**Figure 3A** bottom inset), and neither CD44 nor ezrin were recovered from negative control experiments using non-specific IgG as the immunoprecipitating antibody.

Since interference with raft structure affected interactions between CD44 and ezrin, we next tested the effect of raft disruption on cell migration. Confluent MDA-MB-231 cells exposed to MβCD or vehicle were scratch-wounded and their migration quantitated over time. However MβCD-treated cells in fact migrated slower than untreated cells, with the two slopes showing statistically significant differences (**Figure 3B**, p=0.0144). This potential conflict was explained by immunofluorescence analysis (**Figure 3C**), in which MβCD-treated cells showed increased CD44 and ezrin co-localization throughout the cell membrane rather than specifically at the migrating edge where the interaction could drive migration (**Figure 3C** arrowheads and right panels in the *xz* plane, arrowheads). We hypothesize that the net anti-migratory effect of MβCD may reflect disrupted cellular polarity and impairment of lipid raft-mediated events.

Since the reversible post-translational addition of palmitoyl lipid groups has been shown to promote CD44 localization within rafts [32], we next tested if pharmacological inhibition of depalmitoylation would promote CD44 retention within rafts and consequently decrease CD44/ezrin interactions. MDA-MB-231 cells were co-treated with two de-palmitoylation inhibitors (DPI), methyl arachidonyl fluorophosphate and palmityl trifluoromethyl ketone, and allowed to migrate before analyzing recovery of raft-affiliated versus non-raft-affiliated CD44, flotillin-1 and ezrin (**Figure 4A, left panel**). As before, CD44 mainly localized in lipid raft fractions while ezrin was recovered mainly from non-raft fractions. Given the challenges in defining biochemical fractions / compartments, we devised a novel arithmetic ratio of CD44 in raft fractions to CD44 in non-raft fractions to better describe the movement of CD44 from raft to non-raft compartments and vice-versa. Since traditional loading controls (such as actin) are unequally distributed throughout sucrose density gradient preparations, we had to choose separate loading controls for raft versus non-raft fractions. Flotillin-1 was chosen as a representative loading control strongly enriched in raft fractions, and ezrin as a marker of flotillin-low non-raft fractions. Thus by densitometric quantification of blots exposed for identical periods of time, CD44 expression was normalized to flotillin-1 in order to estimate its abundance in lipid rafts, or to ezrin to estimate its abundance in non-lipid raft fractions. As shown in **Figure 4A** (**graph**), DPI treatment induced a statistically significant increase (nearly 3-fold, $p<0.05$) in the proportion of raft-affiliated CD44 (described by the LR/NR ratio), after DPI treatment. DPI treatment did not alter the raft affiliation of CD44 under non-migrating conditions, further supporting the possibility that CD44 translocation outside lipid rafts is activated only during cell migration.

Having achieved increased retention of CD44 within lipid rafts upon DPI treatment, we next tested whether binding interactions between CD44 and ezrin would consequently be reduced. MDA-MB-231 cells were treated with or without DPI for 30 minutes before induction of migration (**Figure 4B**). As a positive control for increased CD44 and ezrin binding, some cells were treated for 30 minutes with 10mM MβCD prior to the induction of migration. Following wound induction, cells were allowed to migrate in serum-free medium for 30 minutes and immmunoprecipitated for CD44. As already shown (**Figure 1A**), CD44 and ezrin co-precipitation was increased in migrating cells; while disruption of

lipid rafts due to MβCD (**Figure 3A**) significantly increased this binding (p=0.028). Interestingly, DPI treatment, which increased CD44 retention in lipid rafts, virtually abolished the co-precipitation of CD44 and ezrin (**Figure 4B**). Densitometric quantification of CD44 and ezrin binding, normalized to CD44 expression, is shown in **Figure 4B**, **graph**. This was also paralleled by a statistically significant decrease in migration after DPI treatment (**Figure 4C**, p=0.0162).

CD44 localizes outside rafts after induction of CD44-specific migration by ~~on~~ hyaluronic acid

Although scratch wound-induced cell migration was capable of indirectly activating CD44 / ezrin interactions, we also used hyaluronic acid (HA) as a stimulus to directly activate CD44-dependent migration [33], [34]. The concentration of HA (5mg/ml) was chosen on the basis of its ability to promote cell migration in scratch-wounded MDA-MB-231 cells (**Figure 5A**). Since we had previously observed reduced CD44 recovery from lipid rafts after non-specific induction of migration, we hypothesized that CD44-specific migration via HA would induce a similar effect. Confluent MDA-MB-231 cells were scratch-wounded or left stationary and treated with HA for 30 minutes before isolation of raft and non-raft fractions (**Figure 5B**). HA treatment in migrating cells significantly increased the recovery of CD44 ~~in~~ outside lipid raft fractions, compared to non-migrating HA-untreated conditions (**Figure 5B**). However, no significant variations were observed between non-migrating and migrating conditions in the presence of HA treatment. No changes in ezrin, actin and flotillin-1 raft affiliation were observed among the different conditions. These results support the possibility that CD44 is released from lipid rafts during CD44-mediated cancer cell migration [32, 35].

Interference with caveolin-1 or flotillin-1 alone is not sufficient to alter cell migration

Since HA/CD44 binding has been described to be involved in the recycling of CD44 [32] and since their binding has been described to happen in lipid rafts, we have begun to investigate the types of lipid rafts involved in this process. However, although flotillin-1 and caveolin-1 mark two different types of lipid rafts, biochemical separation via sucrose density gradient fractionation cannot easily distinguish between them. In fact caveolin-1 and flotillin-1 were enriched in similar fractions in both migrating and non-migrating MDA-MB-231 cells (**Figure 6A**). We therefore used immunofluorescence studies

to ask whether spatial differences in the localization of either raft marker could shed light on the potential contribution of each raft family to migration in MDA-MB-231 cells. Migrating (M) and non-migrating (NM) cells were double-stained for caveolin-1 or flotillin-1, and examined by confocal microscopy at the basal and suprabasal aspects of the cells (**Figure 6B**). Subtle differences in the basal and suprabasal localization patterns of flotillin-1 and caveolin-1 were observed. For clarity, we define basal pole as the lowest point along the vertical (*xz*) axis, right at the point of attachment to the matrix. This was also the point at which we could clearly see projections (filopodia, lamellipodiae) in the flattened cells at the leading edge of migrating cells. The suprabasal aspect was a higher point along the *xz* axis above the basal pole. We made this distinction to point out that the proteins of interest differentially localize in different planes of the cells.

Specifically, flotillin-1 (green) at the suprabasal aspect of the cells was predominantly enriched in the cell membrane, and its expression levels or distribution did not vary significantly between non-migrating and migrating cells (**Figure 6B**). In contrast, caveolin-1 expression (red) appeared to increase at the suprabasal aspect of migrating relative to non-migrating cells, and its localization was sub-membranous (arrow) in addition to membranous. At the basal pole of MDA-MB-231 cells (the surface at which the cells dynamically attach to and detach from the substratum during migration), there was a strong enrichment of flotillin-1 in the plasma membrane of pseupodial projections in migrating cells (arrowheads). Distribution of caveolin-1 at the basal pole did not vary dramatically between migrating and non-migrating cells, and was again sub-membranous in addition to membranous under both conditions. Overall, there was limited co-localization (yellow) between flotillin-1 and caveolin-1 at either the suprabasal or basal cellular aspects, and no significant changes in co-localization were observed during migration (confirmed by pixel overlap quantification of multiple experiments; data not shown).

These data support the possibility that flotillin-enriched lipid rafts and caveolin-enriched lipid rafts define different subtypes of rafts which could be involved in different cellular processes. Accordingly,

in our hands these raft populations had different subcellular distributions and different patterns of re-localization in MβCD-treated cells compared to controls (**Figure 7**). Specifically, MβCD treatment promoted the enrichment of flotillin-1 but not caveolin-1 staining at the leading edge of migrating cells.

To begin testing the relative involvement of flotillin-1 and caveolin-1 in driving breast cancer cell migration, we also transiently knocked-down the expression of each protein using siRNA technology. After 72h, protein expression of either flotillin-1 or caveolin-1 was successfully reduced by >90% (**Figure 8A**). Immunofluorescence confocal micrographs of flotillin-1 and caveolin-1 further confirmed efficient knockdown of flotillin-1 and caveolin-1 (**Figure 8B**, left and right panels respectively). Surprisingly, analysis of scratch-wound assays revealed that loss of caveolin-1 or flotillin-1 alone was not sufficient to alter cell migration relative to that in cells transfected with negative control siRNA (**Figure 8C**). This likely reflects complexity issues relating to raft crosstalk and also raft-mediated regulation of other proteins involved in migration (besides just CD44). This was supported by double knockdown experiments for flotillin-1 and caveolin-1 (**Figure 8D**), in which the *overall* migratory machinery appears to have been affected. Accordingly, scratch-wound assays revealed that double-knockdown cells migrated significantly less than control or siRNA-ve cells (**Figure 8E**, control vs KD p=0.0125, siRNA-ve vs KD p=0.0092, linear regression, Prism).

Pathway reconstruction

By combining the results shown in **Figure 1A** and **2C** within a logical framework (see methods), we have been able to generate a self-consistent model for the role of lipid rafts in regulating CD44-mediated cell migration (**Figure 9**). This model illustrates the natural biophysical order of processes and is also consistent with the interventions of MβCD, DPI and HA (**Figures 4A, 5B and 6C**). Specifically, it illustrates that CD44 is likely to move outside rafts in order to interact with threonine-phosphorylated (active) ERM and drive migration. The movement of CD44 outside rafts, which is associated with the cell migratory phenotype, is activated by the addition of HA or scratch-wounding, and is inhibited by DPI which cause CD44 to be retained in rafts.

DISCUSSION

CD44 is a highly dynamic molecule involved in many cellular processes, both physiological and pathophysiological. In particular, CD44 and its variants have been described to be altered in many cancers including breast [36]. However, the involvement of CD44 in breast cancer cell migration (an early requirement for metastasis) is still controversial and incompletely understood. Since CD44 is known to localize in cholesterol- and sphingolipid-enriched regions of the cell membrane known as lipid rafts, our study investigated the involvement of rafts in regulating CD44-dependent breast cancer cell migration.

Although the CD44 standard isoform (CD44s) has been described by some as inhibitory towards cell migration [37], others have reported it to be directly involved in breast cancer invasion and tumour progression [38] [39]. The invasive and metastatic breast cell line MDA-MB-231 mainly expressed CD44 with a molecular weight corresponding to that of CD44s (85kDa), and thus was a good model to dissect mechanisms regulating CD44s during breast cancer cell migration. Specifically we were interested to study CD44 regulation of cell migration via its interaction with the cytoskeleton through the linker protein ezrin. Since CD44 and ezrin interactions have been described to regulate wound healing-induced migration [40] and since the migratory pathways activated during wound repair [41] involve the same signalling cascades activated during normal [42] and tumor cell migration [43], scratch-wound assays were used as a model to induce migration of MDA-MB-231 cells. Although CD44 and ezrin interactions during cell migration have been widely described [8, 44], to our knowledge the role of lipid rafts in regulating their interaction during breast cancer cell migration is incompletely understood.

After inducing the migration of confluent MDA-MB-231 cells by scratch-wounding, co-immunoprecipitation experiments revealed a net increase in CD44 and ezrin binding. This implied a conformational change in ezrin to release auto-inhibitory binding between its N- and C-terminal domains [45]. Such conformational changes of ezrin are needed for its binding with CD44, and can be

generated by interactions with lipids (PIP2) or by changes in protein phosphorylation [46]. After induction of cell migration in MDA-MB-231 cells, activation of phosphatidyl-inositol 4-phosphate 5-kinase (PIP5K) has been reported to generate an increase in PIP2 concentration in the internal leaflet of the plasma membrane at the cellular migrating edge [47]. Subsequent interactions between PIP2 and ezrin are then thought to induce plasma membrane localization and activation of ezrin [17, 46]. To act as a cytoskeletal linker, ezrin has not only to acquire an open conformation but also to be phosphorylated at threonine-567, the binding site for F-actin. Protein kinase C (PKC), which is highly active in MDA-MB-231 cells [48], may be responsible for this phosphorylation. In support of these findings, we noted a strong increase in the amount of p-ERM bound to CD44 in migrating cells. This may reflect a combination of p-ezrin, p-radixin and p-moesin, since all three proteins have similar sizes, are expressed in breast cancer cells and their phospho-forms are recognised by the p-ERM antibody. Interestingly, we also observed co-immunoprecipitation between CD44 and a high molecular weight ezrin band (~100kDa). It is intriguing to speculate that this is a product of PKC phosphorylation [49]. Confocal microscopy studies also confirmed CD44 and ezrin co-localization at the migrating edges of MDA-MB-231 cells, with p-ERM mostly localizing at membrane ruffles [50] or in filopodial structures [51] as already reported elsewhere.

Since CD44 has been described to localize to membrane lipid rafts and lipid rafts have been implicated in regulating cancer migration [52], we wondered if rafts could regulate CD44 and ezrin binding by controlling their spatial distribution within cell membranes. Lipid raft extraction from migrating and non-migrating MDA-MB-231 cells revealed that CD44 mainly localized to flotillin1-high lipid raft fractions, although low levels were also detected in flotillin-low non-raft fractions. In contrast, ezrin mainly localized to actin-positive non-raft fractions but was not detected in flotillin-high raft fractions. Prag et al. suggested that non-detection of ezrin in lipid rafts can be due to the low sensitivity of biochemical techniques for the detection of small quantities of ezrin [16], particularly since rafts already have a very low total protein content. Under our conditions, CD44 and ezrin neither co-localized in, nor could be co-immunoprecipitated from, lipid raft fractions under either non-migrating or migrating conditions. However a small pool of non-raft CD44 recovered under migrating conditions co-

precipitated strongly with ezrin, particularly the threonine-phosphorylated (active) form of ERM proteins. It is likely that even a small relative shift of CD44 from raft to non-raft fractions under migratory conditions could permit such an occurrence, and certainly that relative shifts are more important than the absolute presence/absence of CD44 in either raft or non-raft fractions exclusively.

Although the mechanism whereby CD44 is retained in non-raft fractions following the induction of migration is as yet unknown; it is intriguing to speculate that ezrin could sequester CD44 within non-raft fractions after their interaction. Supportive evidence has been drawn from a study in which disruption of the actin cytoskeleton by latrunculin A was found to *increase* CD44 localization within lipid rafts [11]. Since CD44 interacts with actin via linker proteins such as ezrin, this suggests that actin-binding proteins including ezrin may play a major role in the lateral mobility of CD44 outside lipid rafts. However our preliminary experiments showed that ezrin knockdown did not affect CD44 co-localization with flotillin-1-positive lipid rafts (data not shown).

Altogether these findings highlight the dynamic nature of binding interactions between CD44 and ezrin. It has also been described that this binding can be influenced in a time-dependent manner by CD44 phosphorylation status. MDA-MB-231 cells have been shown to possess high levels of PKC activity [48], and *in vitro* studies have shown an increased interaction between CD44 and ezrin up to 40 minutes after PKC activation [8]. At approximately 40 minutes, a second phosphorylation event on Serine-291 of CD44 reportedly generates conformational changes that decrease CD44 and ezrin affinity [8]. Therefore we examined CD44 and ezrin interactions after 30 minutes from induction of migration, supposedly before CD44 and ezrin disengage (estimated at 40 minutes after the induction of migration). Results generated using this migration model provided novel information to suggest that the interactions between CD44 and ezrin occur outside lipid rafts. Although we did not directly test CD44/ezrin interactions at later timepoints, our co-localization data and the results of Legg et al.[8] suggest that CD44/ezrin interactions outside lipid rafts most likely occur during the early stages of migration.

Our hypothesis that CD44 and ezrin interact outside lipid raft domains was further supported by experiments in which CD44-specific migration was directly stimulated by exposure to its extracellular matrix ligand HA. This stimulated a significant increase in CD44 localization outside lipid rafts in migrating HA-treated cells compared to non-migrating HA-untreated conditions. It should also be noted that there are many different types of HA fragments, and it is possible that other fragments could induce a greater translocation of CD44 outside of rafts. It has been described that HA interactions with CD44 are necessary for HA recycling and degradation [35] in tumour cell migration [53]. It is possible that CD44 detection in non-raft fractions after induction of migration could correlate with CD44 internalization into membrane-enclosed vesicles, as has already been described in association with HA degradation. To further support this hypothesis, we found decreased levels of CD44 in single planes of the cell membrane at 120 minutes after induction of migration. In fact CD44 recycling has already been described as a necessary event in cell migration [54]. Additionally, we observed that in non-migrating HA-treated cells, CD44 recovery outside lipid rafts was not significantly different from that in other conditions (non-migrating HA-treated, migrating HA-treated/-untreated). This may suggest that HA treatment in non-migrating conditions induces changes at the molecular level intermediate between migrating and non-migrating phenotypes. It is possible that, following HA stimulation in non-migrating conditions, CD44 can only be partially internalized since contact-inhibited cells cannot properly migrate. This might preclude any further CD44 internalization. Moreover, depending on the size of its particles, HA treatment could cause CD44 clustering, thereby bringing together lipid rafts and increasing CD44 detergent insolubility[11]. This intermediate phenotype may help explain the lack of statistically-significant differences between CD44 raft/non-raft segregation in HA-treated versus – untreated non-migrating cells, or in HA-treated non-migrating versus migrating cells. Specifically endocytosis can be a possible mechanism involved in CD44 recycling and it has been described to be inhibited by MβCD treatments [52]. Therefore we speculate that enhanced binding between ezrin (total or active) and CD44 after MβCD treatment may be due to a block in the endocytotic pathway inhibiting CD44 and ezrin from disengaging and resulting in an increased interaction between the two. Accordingly, immunofluorescence analysis of CD44 and ezrin after lipid raft disruption confirmed their enhanced localization throughout cell membranes. However, since lipid rafts carry out many

important regulatory functions, extensive raft disruption due to MβCD may also interfere with other key cellular functions including regulation of cell polarity. It should also be noted that MβCD, although widely accepted as a pharmacological disrupter of lipid rafts [21-23], is non-specific in this regard. Therefore our crude evidence of MβCD-induced raft disruption facilitating CD44/ezrin interactions could be better refined, should more selective and specific raft-disruptive reagents become available in the future.

To further test the potential spatial control of lipid rafts over CD44/ezrin interactions, we have begun to explore the possibility of pharmacologically inhibiting the departure of CD44 from rafts using protein palmitoylation inhibitors. CD44 has two conserved cysteine residues that can be palmitoylated [32]; a post-translational modification which increases its hydrophobicity and affinity for lipid raft domains. In turn, lipid raft proteins, such as CD44, can be dynamically de-palmitoylated by the action of palmitoyl protein thioesterases [55], which decrease their affinity for lipid rafts. Moreover, phosphorylation events, such as those described during cell migration, can induce conformational changes that also affect the exposure of the palmitoylation sites and therefore regulate protein localization to lipid rafts [56]. Using a combination of depalmitoylation inhibitors (DPI) to prevent depalmitoylation, we successfully inhibited the release of a pool of CD44 from lipid rafts. The net effect of forced detainment of CD44 within rafts was that CD44 / ezrin co-precipitation was practically abolished. This was paralleled by reduced cell migration, supporting our hypothesis that lipid rafts exert a key regulatory influence on CD44 / ezrin interactions and subsequently cell migration. This finding also supports the idea that CD44 and ezrin binding is very dynamic and that the relative spatial localization of these two proteins can play an important role in regulating the physiology of binding. However DPI represent a class of non-selective inhibitors about which little is known, thus the observed functional effects in our exploratory experiments cannot at this time be attributed solely to changes in CD44 palmitoylation status. Since CD44 localization to lipid rafts is due to CD44 palmitoylation on specific cysteines, this represents a logical future strategy to better interrogate the specific contribution of CD44 palmitoylation changes to the functional modulation of cell migration. We speculate that phosphorylation events during cell migration may induce

conformational changes in CD44 that mask its palmitoylation sites, decreasing CD44 affinity for lipid rafts. We suggest that this may be a possible mechanism involved in the control of CD44/ezrin relocation outside lipid rafts during breast cancer cell migration. However further studies are needed to assess this mechanism.

Many different types of lipid rafts have been described to play roles in cell migration. Flotillin-1 and caveolin-1 represent two key markers of different raft populations. Our studies in MDA-MB-231 cells suggest that CD44 predominantly associates with flotillin-positive rather than caveolin-positive rafts. Immunofluorescence analysis also confirmed that caveolin-1 knockdown does not significantly alter CD44 and flotillin-1 colocalization during migration (data not shown), supporting our hypothesis that CD44-dependent cell migration is not under direct regulatory control by caveolin-positive lipid rafts. Accordingly, recent publications describe CD44 as a carrier in non-caveolar, clathrin-independent pathways in mouse embryonic fibroblasts [54]. Interestingly however, transient knockdown of neither flotillin-1 nor caveolin-1 was sufficient to alter cell migratory characteristics over a short timecourse in our scratch-wound migration assays relative to a negative control siRNA. Although an increase in migration might have been expected under flotillin-knockdown conditions if CD44 was indeed being released from rafts and becoming free to interact with ezrin, it must be remembered that lipid rafts are highly complex structures which regulate the location and function of many cellular proteins. Several such proteins (including key kinases and focal adhesion proteins, including Src and FAK) are known to play key roles in cell migration [57]. Therefore there are likely to be compensatory mechanisms which act to preserve important cellular functions (such as migration) even in the event of raft loss. Spatial and temporal considerations must also be taken into account, since stable loss of caveolin-1 has been reported to reduce invasive behavior in breast cancer cells over a longer timescale[58]. Accordingly, long-term loss of caveolin-1 has been described to be associated with cell transformation and tumoral growth[59]. Furthermore, potential cross-talk between flotillin-1 and caveolin-1 may also impact cell functional behaviour. For example, in intestinal epithelial cells, flotillin-1 down-regulation has been reported to down-regulate caveolin-1 availability by preventing its lysosomal degradation[60]. In fact, scratch wound assays revealed that cells doubly-knocked down for flotillin-1 and caveolin-1 migrated

significantly less than control or siRNA-ve cells, further supporting the hypothesis that an organized lipid raft machinery is needed to allow functional cell migration. We speculate that the complete loss of rafts may inflict a global dysregulation upon cell migration via the uncoupling of various signalling pathways which depend on raft/non-raft segregation of effector components. Overall, our studies highlight that the regulation of CD44-dependent cell migration by either flotillin-positive or caveolin-positive lipid rafts is complex, and will require very specific experimental approaches in the future to dissect the relative roles of each type of raft population (as well as their crosstalk).

Taken together, our observations have shed novel light on the role of lipid rafts in regulating CD44-mediated cell migration. It is interesting to note that our surface area calculations estimated only <10% of cells to be migrating at any one time, despite our extensive scratch-wounding protocol. This calculation is only a crude physical approximation of the number of migrating cells at 30 minutes after stimulation. Based on immunofluorescent observations of flattened cells, we estimated that four-five cells back from each wound edge were likely to be actively migrating. However it is known that even cells *behind* the migrating edge are also affected by wounding. Indeed injured epithelial cells release ATP and different chemotactic factors into culture medium *in vitro*, thereby activating calcium waves that trigger different early responses through activation of ADAMs and EGF receptors, both of which are involved in the activation of migratory pathways[29]. This suggests that our estimate of only <10% cell migration is very conservative, and could explain why statistically significant differences in sub-membranous trafficking of CD44 and its interactions with ezrin were detected even at such low levels of migration. Since only small numbers of cells are likely to migrate out of a tumor during early invasion and metastasis, it is intriguing to speculate that our mechanism is biologically relevant to that scenario. However *in vivo* experimentation would be necessary to better investigate the real relevance to tumor metastasis. Using experimental data to construct a logical framework based on our *in vitro* data, we propose a model (**Figure 9**) whereby lipid rafts regulate interactions between CD44 with ezrin in its active (phosphorylated) form in order to orchestrate breast cancer cell migration. Specifically, in the stationary state CD44 is mostly retained within rafts and unable to interact with phospho-ERM proteins to drive migration. Upon exposure to a migratory stimulus (such as non-

specific wounding or CD44-specific stimulation with HA), CD44 moves out of rafts, potentially following its depalmitoylation, and is free to interact with activated ERM proteins. This is then associated with the migratory phenotype. We speculate that further exploration of mechanisms to specifically target and modulate CD44 localization to lipid rafts may have value for the long-term development of new anti-migratory breast cancer treatments.

REFERENCES

1. Sherman L, Sleeman J, Dall P, Hekele A, Moll J, Ponta H, Herrlich P: The CD44 proteins in embryonic development and in cancer, Curr Top Microbiol Immunol 1996, 213 (Pt 1):249-269
2. Lin L, Cheung AW, Chan SO: Chiasmatic neurons in the ventral diencephalon of mouse embryos--changes in arrangement and heterogeneity in surface antigen expression, Brain Res Dev Brain Res 2005, 158:1-12
3. Haynes BF, Telen MJ, Hale LP, Denning SM: CD44--a molecule involved in leukocyte adherence and T-cell activation, Immunol Today 1989, 10:423-428
4. Smadja-Joffe F, Legras S, Girard N, Li Y, Delpech B, Bloget F, Morimoto K, Le Bousse-Kerdiles C, Clay D, Jasmin C, Levesque JP: CD44 and hyaluronan binding by human myeloid cells, Leuk Lymphoma 1996, 21:407-420, color plates following 528
5. Wang C, Tammi M, Tammi R: Distribution of hyaluronan and its CD44 receptor in the epithelia of human skin appendages, Histochemistry 1992, 98:105-112
6. Heldin P, Karousou E, Bernert B, Porsch H, Nishitsuka K, Skandalis SS: Importance of hyaluronan-CD44 interactions in inflammation and tumorigenesis, Connect Tissue Res 2008, 49:215-218
7. Weber GF, Ashkar S, Cantor H: Interaction between CD44 and osteopontin as a potential basis for metastasis formation, Proc Assoc Am Physicians 1997, 109:1-9
8. Legg JW, Lewis CA, Parsons M, Ng T, Isacke CM: A novel PKC-regulated mechanism controls CD44 ezrin association and directional cell motility, Nat Cell Biol 2002, 4:399-407
9. Matsui T, Maeda M, Doi Y, Yonemura S, Amano M, Kaibuchi K, Tsukita S, Tsukita S: Rho-kinase phosphorylates COOH-terminal threonines of ezrin/radixin/moesin (ERM) proteins and regulates their head-to-tail association, J Cell Biol 1998, 140:647-657
10. Carter WG, Wayner EA: Characterization of the class III collagen receptor, a phosphorylated, transmembrane glycoprotein expressed in nucleated human cells, J Biol Chem 1988, 263:4193-4201
11. Oliferenko S, Paiha K, Harder T, Gerke V, Schwarzler C, Schwarz H, Beug H, Gunthert U, Huber LA: Analysis of CD44-containing lipid rafts: Recruitment of annexin II and stabilization by the actin cytoskeleton, J Cell Biol 1999, 146:843-854
12. Helms JB, Zurzolo C: Lipids as targeting signals: lipid rafts and intracellular trafficking, Traffic 2004, 5:247-254
13. Patra SK: Dissecting lipid raft facilitated cell signaling pathways in cancer, Biochim Biophys Acta 2008, 1785:182-206
14. Orian-Rousseau V: CD44, a therapeutic target for metastasising tumours, Eur J Cancer 2010, 46:1271-1277
15. Lajoie P, Nabi IR: Lipid rafts, caveolae, and their endocytosis, Int Rev Cell Mol Biol 2010, 282:135-163
16. Prag S, Parsons M, Keppler MD, Ameer-Beg SM, Barber P, Hunt J, Beavil AJ, Calvert R, Arpin M, Vojnovic B, Ng T: Activated ezrin promotes cell migration through recruitment of the GEF Dbl to lipid rafts and preferential downstream activation of Cdc42, Mol Biol Cell 2007, 18:2935-2948
17. Hirao M, Sato N, Kondo T, Yonemura S, Monden M, Sasaki T, Takai Y, Tsukita S, Tsukita S: Regulation mechanism of ERM (ezrin/radixin/moesin) protein/plasma membrane association: possible involvement of phosphatidylinositol turnover and Rho-dependent signaling pathway, J Cell Biol 1996, 135:37-51

18. Barret C, Roy C, Montcourrier P, Mangeat P, Niggli V: Mutagenesis of the phosphatidylinositol 4,5-bisphosphate (PIP(2)) binding site in the NH(2)-terminal domain of ezrin correlates with its altered cellular distribution, J Cell Biol 2000, 151:1067-1080
19. Johnson CM, Rodgers W: Spatial Segregation of Phosphatidylinositol 4,5-Bisphosphate (PIP(2)) Signaling in Immune Cell Functions, Immunol Endocr Metab Agents Med Chem 2008, 8:349-357
20. Kojic LD, Joshi B, Lajoie P, Le PU, Cox ME, Turbin DA, Wiseman SM, Nabi IR: Raft-dependent endocytosis of autocrine motility factor is phosphatidylinositol 3-kinase-dependent in breast carcinoma cells, J Biol Chem 2007, 282:29305-29313
21. Ortiz-Ferron G, Yerbes R, Eramo A, Lopez-Perez AI, De Maria R, Lopez-Rivas A: Roscovitine sensitizes breast cancer cells to TRAIL-induced apoptosis through a pleiotropic mechanism, Cell Res 2008, 18:664-676
22. Simons K, Toomre D: Lipid rafts and signal transduction, Nat Rev Mol Cell Biol 2000, 1:31-39
23. Awasthi V, Mandal SK, Papanna V, Rao LV, Pendurthi UR: Modulation of tissue factor-factor VIIa signaling by lipid rafts and caveolae, Arterioscler Thromb Vasc Biol 2007, 27:1447-1455
24. Bowie RV, Donatello S, Lyes C, Owens MB, Babina IS, Hudson L, Walsh SV, O'Donoghue DP, Amu S, Barry SP, Fallon PG, Hopkins AM: Lipid rafts are disrupted in mildly-inflamed intestinal microenvironments without overt disruption of the epithelial barrier, Am J Physiol Gastrointest Liver Physiol
25. Nusrat A, Parkos CA, Verkade P, Foley CS, Liang TW, Innis-Whitehouse W, Eastburn KK, Madara JL: Tight junctions are membrane microdomains, J Cell Sci 2000, 113 (Pt 10):1771-1781
26. Kyoda KM, Morohashi M, Onami S, Kitano H: A gene network inference method from continuous-value gene expression data of wild-type and mutants, Genome Inform Ser Workshop Genome Inform 2000, 11:196-204
27. Tsukita S, Oishi K, Sato N, Sagara J, Kawai A, Tsukita S: ERM family members as molecular linkers between the cell surface glycoprotein CD44 and actin-based cytoskeletons, J Cell Biol 1994, 126:391-401
28. Farooqui R, Fenteany G: Multiple rows of cells behind an epithelial wound edge extend cryptic lamellipodia to collectively drive cell-sheet movement, J Cell Sci 2005, 118:51-63
29. Yin J, Xu K, Zhang J, Kumar A, Yu FS: Wound-induced ATP release and EGF receptor activation in epithelial cells, J Cell Sci 2007, 120:815-825
30. Chen Y, Wang D, Guo Z, Zhao J, Wu B, Deng H, Zhou T, Xiang H, Gao F, Yu X, Liao J, Ward T, Xia P, Emenari C, Ding X, Thompson W, Ma K, Zhu J, Aikhionbare F, Dou K, Cheng SY, Yao X: Rho kinase phosphorylation promotes ezrin-mediated metastasis in hepatocellular carcinoma, Cancer Res 2011, 71:1721-1729
31. Milhiet PE, Giocondi MC, Baghdadi O, Ronzon F, Roux B, Le Grimellec C: Spontaneous insertion and partitioning of alkaline phosphatase into model lipid rafts, EMBO Rep 2002, 3:485-490
32. Thankamony SP, Knudson W: Acylation of CD44 and its association with lipid rafts are required for receptor and hyaluronan endocytosis, J Biol Chem 2006, 281:34601-34609
33. Bourguignon LY, Zhu H, Shao L, Chen YW: CD44 interaction with tiam1 promotes Rac1 signaling and hyaluronic acid-mediated breast tumor cell migration, J Biol Chem 2000, 275:1829-1838
34. Bourguignon LY, Zhu H, Zhou B, Diedrich F, Singleton PA, Hung MC: Hyaluronan promotes CD44v3-Vav2 interaction with Grb2-p185(HER2) and induces Rac1 and Ras

signaling during ovarian tumor cell migration and growth, J Biol Chem 2001, 276:48679-48692
35. Knudson W, Chow G, Knudson CB: CD44-mediated uptake and degradation of hyaluronan, Matrix Biol 2002, 21:15-23
36. Iida N, Bourguignon LY: New CD44 splice variants associated with human breast cancers, J Cell Physiol 1995, 162:127-133
37. Ilangumaran S, Hoessli DC: Effects of cholesterol depletion by cyclodextrin on the sphingolipid microdomains of the plasma membrane, Biochem J 1998, 335 (Pt 2):433-440
38. Afify A, McNiel MA, Braggin J, Bailey H, Paulino AF: Expression of CD44s, CD44v6, and hyaluronan across the spectrum of normal-hyperplasia-carcinoma in breast, Appl Immunohistochem Mol Morphol 2008, 16:121-127
39. Hill A, McFarlane S, Mulligan K, Gillespie H, Draffin JE, Trimble A, Ouhtit A, Johnston PG, Harkin DP, McCormick D, Waugh DJ: Cortactin underpins CD44-promoted invasion and adhesion of breast cancer cells to bone marrow endothelial cells, Oncogene 2006, 25:6079-6091
40. Jensen PV, Larsson LI: Actin microdomains on endothelial cells: association with CD44, ERM proteins, and signaling molecules during quiescence and wound healing, Histochem Cell Biol 2004, 121:361-369
41. Fenteany G, Janmey PA, Stossel TP: Signaling pathways and cell mechanics involved in wound closure by epithelial cell sheets, Curr Biol 2000, 10:831-838
42. Ridley AJ, Schwartz MA, Burridge K, Firtel RA, Ginsberg MH, Borisy G, Parsons JT, Horwitz AR: Cell migration: integrating signals from front to back, Science 2003, 302:1704-1709
43. Dvorak HF: Tumors: wounds that do not heal. Similarities between tumor stroma generation and wound healing, N Engl J Med 1986, 315:1650-1659
44. Yonemura S, Hirao M, Doi Y, Takahashi N, Kondo T, Tsukita S, Tsukita S: Ezrin/radixin/moesin (ERM) proteins bind to a positively charged amino acid cluster in the juxta-membrane cytoplasmic domain of CD44, CD43, and ICAM-2, J Cell Biol 1998, 140:885-895
45. Jayaraman B, Nicholson LK: Thermodynamic dissection of the Ezrin FERM/CERMAD interface, Biochemistry 2007, 46:12174-12189
46. Fievet BT, Gautreau A, Roy C, Del Maestro L, Mangeat P, Louvard D, Arpin M: Phosphoinositide binding and phosphorylation act sequentially in the activation mechanism of ezrin, J Cell Biol 2004, 164:653-659
47. Yamaguchi H, Yoshida S, Muroi E, Kawamura M, Kouchi Z, Nakamura Y, Sakai R, Fukami K: Phosphatidylinositol 4,5-bisphosphate and PIP5-kinase Ialpha are required for invadopodia formation in human breast cancer cells, Cancer Sci 2010, 101:1632-1638
48. Platet N, Prevostel C, Derocq D, Joubert D, Rochefort H, Garcia M: Breast cancer cell invasiveness: correlation with protein kinase C activity and differential regulation by phorbol ester in estrogen receptor-positive and -negative cells, Int J Cancer 1998, 75:750-756
49. Ng T, Parsons M, Hughes WE, Monypenny J, Zicha D, Gautreau A, Arpin M, Gschmeissner S, Verveer PJ, Bastiaens PI, Parker PJ: Ezrin is a downstream effector of trafficking PKC-integrin complexes involved in the control of cell motility, Embo J 2001, 20:2723-2741
50. Bretscher A: Rapid phosphorylation and reorganization of ezrin and spectrin accompany morphological changes induced in A-431 cells by epidermal growth factor, J Cell Biol 1989, 108:921-930
51. Nakamura N, Oshiro N, Fukata Y, Amano M, Fukata M, Kuroda S, Matsuura Y, Leung T, Lim L, Kaibuchi K: Phosphorylation of ERM proteins at filopodia induced by Cdc42, Genes Cells 2000, 5:571-581

52. Liu Y, Sun R, Wan W, Wang J, Oppenheim JJ, Chen L, Zhang N: The involvement of lipid rafts in epidermal growth factor-induced chemotaxis of breast cancer cells, Mol Membr Biol 2007, 24:91-101
53. Knudson W: The role of CD44 as a cell surface hyaluronan receptor during tumor invasion of connective tissue, Front Biosci 1998, 3:d604-615
54. Howes MT, Kirkham M, Riches J, Cortese K, Walser PJ, Simpson F, Hill MM, Jones A, Lundmark R, Lindsay MR, Hernandez-Deviez DJ, Hadzic G, McCluskey A, Bashir R, Liu L, Pilch P, McMahon H, Robinson PJ, Hancock JF, Mayor S, Parton RG: Clathrin-independent carriers form a high capacity endocytic sorting system at the leading edge of migrating cells, J Cell Biol 2010, 190:675-691
55. Goswami R, Ahmed M, Kilkus J, Han T, Dawson SA, Dawson G: Differential regulation of ceramide in lipid-rich microdomains (rafts): antagonistic role of palmitoyl:protein thioesterase and neutral sphingomyelinase 2, J Neurosci Res 2005, 81:208-217
56. Salaun C, Greaves J, Chamberlain LH: The intracellular dynamic of protein palmitoylation, J Cell Biol 191:1229-1238
57. Babina I, Donatello S, Nabi I, Hopkins A: Lipid rafts as master regulators of breast cancer cell function. Edited by Gunduz M, Gunduz E. InTech, 2011, p.
58. Joshi B, Strugnell SS, Goetz JG, Kojic LD, Cox ME, Griffith OL, Chan SK, Jones SJ, Leung SP, Masoudi H, Leung S, Wiseman SM, Nabi IR: Phosphorylated caveolin-1 regulates Rho/ROCK-dependent focal adhesion dynamics and tumor cell migration and invasion, Cancer Res 2008, 68:8210-8220
59. Galbiati F, Volonte D, Engelman JA, Watanabe G, Burk R, Pestell RG, Lisanti MP: Targeted downregulation of caveolin-1 is sufficient to drive cell transformation and hyperactivate the p42/44 MAP kinase cascade, EMBO J 1998, 17:6633-6648
60. Vassilieva EV, Ivanov AI, Nusrat A: Flotillin-1 stabilizes caveolin-1 in intestinal epithelial cells, Biochem Biophys Res Commun 2009, 379:460-465

FIGURE LEGENDS

Figure 1. CD44 and ezrin interaction during breast cancer cell migration.

(A) CD44 was immunoprecipitated from equal amounts of total protein extracted from migrating (M) and non-migrating (NM) MDA-MB-231 cells. Increased binding between CD44 and ezrin was observed in migrating conditions but no changes in p-threonine-ERM (p-ERM) binding to CD44 were observed (graph, error bars refer to the SEM of three independent experiments with unpaired two-tailed t-tests used for statistical analysis). Blots from input lysates (right inset) confirm similar expression levels of CD44, p-ERM, ezrin and actin in both treatment conditions. Immunofluorescence analysis of CD44 and ezrin **(B**, green and red respectively) or CD44 and p-ERM (**C**, green and red respectively) co-localization (yellow, merge) in non-migrating (NM) and migrating (M) MDA-MB-231 cells. A significant increase in CD44 and ezrin co-localization was observed in migrating compared to non-migrating cells (**B**, graph, unpaired two-tailed t-test, p=0.0108, error bars represent SEM of two independent experiments), especially at the leading edge of migrating cells (**B**, inset). A non-significant increase of CD44 and p-ERM co-localization was also observed (**C** graph, white bars). Interestingly increased expression and localization of p-ERM in membrane ruffles at the migrating edge was described over time in cell migration together with a total increase in p-ERM expression (**C**, arrowheads at 30 min and at 120 min, graph, grey bars). Conversely, a decrease of total CD44 expression was observed over time (graph, black bars). Error bars refer to the SEM of duplicate experiments.

Figure 2. CD44 and ezrin localization to lipid rafts during breast cancer cell migration.

(A) Lipid rafts were isolated from migrating and non-migrating MDA-MB-231 cells via isopycnic sucrose density gradient fractionation, and successive fractions analyzed for activity of the raft marker enzyme alkaline phosphatase, protein concentration or sucrose density. **(B)** Equivalent protein concentrations from gradient fractions were separated by SDS-PAGE and analyzed by Western blotting for the expression of CD44, flotillin-1, ezrin and actin. The amount of CD44 present in lipid raft versus non-raft fractions was significantly higher (unpaired two-tailed t-test, p=0.036) in non-migrating compared to migrating cells (graph, error bar refers to SEM of triplicate experiments). **(C)**

Equal amounts of total cellular protein from lipid raft and non-lipid raft fractions of migrating and non-migrating MDA-MB-231 cells were immunoprecipitated for CD44 and probed for CD44, ezrin and p-threonine-ERM (one replicate). Due to strong differences in CD44 levels between raft and non-raft fractions, western blots of two different exposure times are given: short exposure times for lipid raft fractions (left panel) and longer exposure times for non-raft fractions (right panel). Blots from input lysates (far right; same exposure time) confirmed much higher expression of CD44 in raft compared to non-raft fractions together with ezrin enrichment in non-raft fractions, irrespective of cell migratory status. CD44 recovery from lipid raft fractions was decreased in migrating cells compared to non-migrating cells, and CD44/ezrin co-precipitation was observed predominantly in non-lipid raft fractions of migrating cells. (**D**) MDA-MB-231 cells were transfected with siRNA against the principal structural components of different lipid raft populations, flotillin-1 or caveolin-1. Migrating versus non-migrating cells were subsequently analyzed by immunofluorescence confocal microscopy for CD44 co-localization with either moesin (top panel) or radixin (bottom panel), which was quantitated with Image J software. Flotillin-1 knockdown significantly decreased the co-localization of CD44 and moesin (unpaired two-tailed t-test, p= 0.0027) while significantly increasing the co-localization of CD44 and radixin (unpaired two-tailed t-test, p= 0.0247, error bars refers to SEM of representative triplicate images).

Figure 3. Disruption of lipid rafts alters CD44/ezrin interactions and cell migratory capabilities. **(A)** CD44 was immunoprecipitated from equal amounts of total cellular protein isolated from MDA-MB-231 cells treated with 10mM MβCD (or vehicle) for 30 minutes in serum-free medium prior to the induction of cell migration for 30 minutes (top panel). Following MβCD treatment, CD44 and ezrin binding was significantly increased compared to that in control untreated cells (graph, error bars refer to SEM of 3 replicate experiments, unpaired two-tailed t-test,p=0.0412). Blots from input lysates (bottom inset) confirm similar expression levels of CD44 in both treatment conditions. **(B)** The effect of MβCD on MDA-MB-231 cell migration was tested by scratch wound assay. Cells treated with 10 mM MβCD for 30 minutes showed significant impairments in cell migration over time (error bars refer to SEM of n=5 experiments, GraphPad Prism linear regression analysis, p=0.0144). **(C)**

Immunofluorescence detection of CD44 (green) and ezrin (red) in non-migrating cells or during cell migration in non treated cell (control) and in cells treated with 10 mM MβCD for 30 minutes (left panels). After MβCD treatment, confocal imaging in the *xz* plane (right panels) revealed extensive co-localization of CD44/ezrin throughout the membranes of cells both at the leading and trailing edges of migrating cell sheets (arrowheads).

Figure 4. Forced CD44 affiliation with lipid rafts disrupts CD44 and ezrin binding and cell migratory abilities.

(A) MDA-MB-231 cells were treated with depalmitoylation inhibitors (DPI; 5µM methyl arachidonyl fluorophosphate and 20µM palmityl trifluoromethyl ketone) or vehicle for 30 minutes, and either induced to migrate or left stationary for 30 minutes in serum-free medium. Cells were extracted for lipid raft isolation with 1% Triton X-100 and analyzed by SDS-PAGE and Western blotting for expression of CD44, flotillin-1 and ezrin. CD44 within lipid raft fractions was normalized to flotillin-1 expression while non-raft CD44 was normalized to ezrin expression. The relative amount of CD44 in lipid rafts was given by the LR/NR ratio (graph on the right). A significant increase in CD44 localization to lipid rafts in migrating cells was observed after DPI treatment (unpaired two-tailed t-test, p=0.0331, error bars refer to SEM of duplicate experiments), while no changes in ezrin localization were observed after DPI treatment. **(B)** Ezrin and CD44 binding was analyzed in non-migrating (NM) or migrating (M) MDA-MB-231 cells treated for 30 minutes with 10mM MβCD or a combination of the DPIs 5µM methyl arachidonyl fluorophosphate and 20µM palmityl trifluoromethyl ketone (DPI) in serum-free medium. After treatment, cells were immunoprecipitated for CD44 and probed for ezrin. Band quantification is presented on the right. Compared to control conditions, MβCD treatment significantly increased CD44 / ezrin co-precipitation (unpaired two-tailed t-test, p=0.028, error bars refer to SEM of triplicate experiments) while DPI greatly decreased CD44 / ezrin co-precipitation. **(C)** The effect of DPI treatment on MDA-MB-231 cell migration was tested by scratch wound assay. Cells were pre-treated with a combination of 5µM methyl arachidonyl fluorophosphate and 20µM palmityl trifluoromethyl ketone (DPI) or vehicle for 30 minutes and then scratch-wounded. Wound closure was measured over time up to 9h (error bars refer to SEM of duplicate experiments,

with multiple replicates per experiment). DPI treatment significantly slowed wound closure compared to control conditions (GraphPad Prism linear regression analysis, p=0.0162).

Figure 5: HA-stimulated migration in MDA-MB-231 cells is associated with reductions in raft-affiliated CD44.

(A) After wounding, MDA-MB-231 cells were stimulated with 5mg/ml HA (+HA) or serum-free medium alone (-HA) and allowed to migrate for up to 8 hours. Wound closure was measured over time. HA treatment promoted wound closure approximately two-fold more than control conditions and linear regression analysis confirmed a statistical difference between the two curves (GraphPad Prism linear regression analysis, p=0.005, error bars refer to SEM of triplicate experiments). **(B)** MDA-MB-231 cells were stimulated with 5mg/ml HA or with vehicle alone, and scratch-wounded (migrating, M) or left stationary (non-migrating, NM). Cells were separated into lipid raft and non- raft fractions by ultracentrifugation on sucrose gradients and each fraction analyzed by SDS-PAGE for CD44, ezrin, flotillin-1 and actin expression. CD44 localization to lipid raft (LR) versus non-lipid raft fractions (NR) in the different conditions, expressed as LR/NR ratio, is shown in the graph at the bottom (error bars refer to the SEM of 3 experiments). There was a statistically significant reduction in CD44 recovery from rafts under HA-treated or -untreated migrating conditions compared to HA-untreated non-migrating conditions (unpaired two-tailed t-test, HA-: p=0.031; HA+: p=0.014).

Figure 6: Flotillin-positive lipid rafts and caveolin-positive lipid rafts have different subcellular localizations.

(A) Lipid rafts were isolated from migrating (M) or non-migrating (NM) MDA-MB-231 cells and immunoblotted for flotillin-1 and caveolin-1. Both flotillin-1 and caveolin-1 localized in the same fractions harvested from sucrose density gradients. **(B)** MDA-MB-231 cells were analyzed by immunofluorescence confocal microscopy for flotillin-1 (green) and caveolin-1 (red) co-localization at either the suprabasal or basal aspects of the cells. Flotillin-1 was strongly enriched in protrusive structures at the basal aspect of migrating cells. Three confocal micrographs containing three - five cells each were analyzed.

Figure 7: MβCD treatment differentially affects caveolin-1 and flotillin-1 localization in the cell compartment.

MDA-MB-231 cells were treated with 10mM MβCD or vehicle (Control) for 30 minutes and then induced to migrate. Cells were then were analyzed by immunofluorescence confocal microscopy for caveolin-1 (red) and flotillin-1 (green) co-localization at either the suprabasal or basal aspect of the cells. Three confocal micrographs containing three - five cells each were analyzed. Following MβCD treatment, flotillin-1 presented a different reorganization between the suprabasal and basal aspects while caveolin-1 was distributed relatively uniformly throughout the cells. This may suggest differential functions of lipid rafts identified by caveolin-1 compared to those identified by flotillin-1.

Figure 8: Knockdown of flotillin-1 and caveolin-1 does not alter cell migration in MDA-MB-231.

siRNA against flotillin-1 and/or caveolin-1 or a universal negative control siRNA was used to transiently knockdown gene expression in MDA-MB-231 cells for 72h before performing migration assays or immunofluorescence analysis. **(A)** After 72h the efficiency of transfection was checked by SDS-PAGE and Western blotting analysis. Expression of flotillin-1 and caveolin-1 alone was successfully reduced by approximately 90%. (**B**) Decreased expression of flotillin-1 (left panel) and caveolin-1 (right panel) following siRNA knockdown was also confirmed by immunofluorescence confocal microscopy. (**C**) Analysis of scratch-wound assays between knockdown conditions (relative to that in cells transfected with the negative control siRNA) did not reveal any significant differences in cell migration. (**D**) The efficiency of simultaneous knockdown of flotillin-1 and caveolin-1 after 72h from transfection was tested by Western blot analysis of flotillin-1 and caveolin-1 expression. (**E**) Analysis of scratch-wound assays of cells double knocked-down for flotillin-1 and caveolin-1 revealed significantly less cell migration than in untreated cells or those transfected with the negative control siRNA (linear regression analysis, GraphPad Prism, p(●vs▼)=0.0125, p(○vs▼)=0.0092p.

Figure 9: Lipid raft-mediated CD44 and ezrin interaction model.

The CD44 cell migration pathway reconstructed using immunoprecipitation experiments and logical modelling. Horizontal arrows indicate the resulting flux when transiting from a stationary to migratory cell phenotype. Our model suggests that the transit between a stationary and migratory state is associated with release of CD44 from lipid rafts (possibly via de-palmitoylation), whereupon non-raft CD44 can bind phosphorylated (active) ezrin in order to initiate migration.

Figure 1

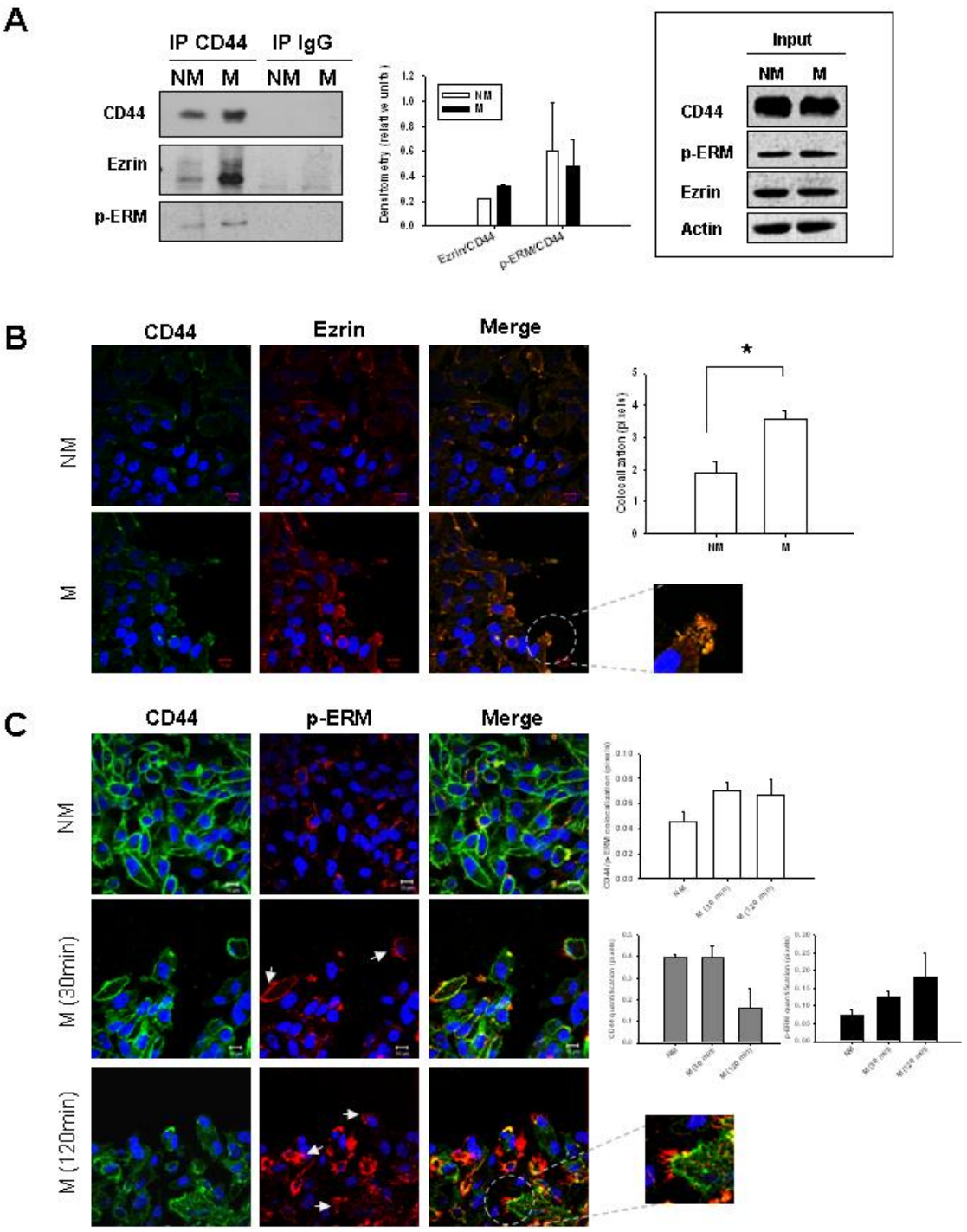
A
IP CD44
IP IgG
NM M NM M
CD44
Ezrin
p-ERM
Densitometry (relative units)
NM
M
Ezrin/CD44
p-ERM/CD44
Input
NM M
CD44
p-ERM
Ezrin
Actin
B
CD44
Ezrin
Merge
NM
M
*
Colocalization (pixels)
NM
M
C
CD44
p-ERM
Merge
NM
M (30min)
M (120min)

Figure 2

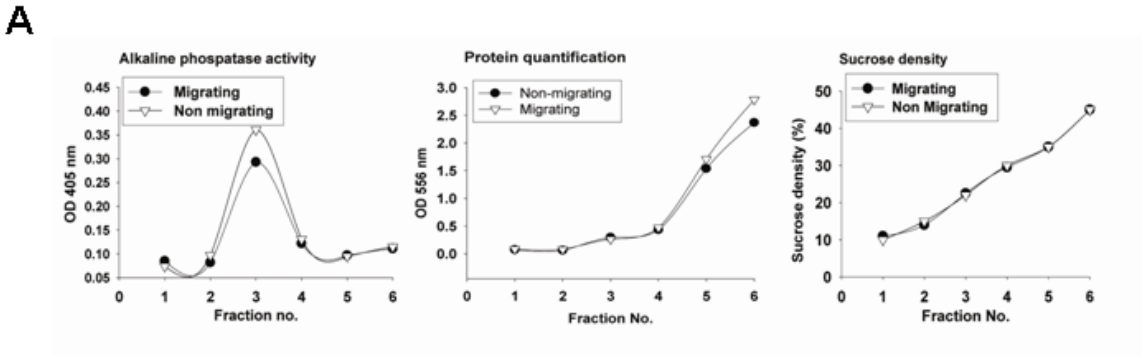
A
Alkaline phospatase activity
Migrating
Non migrating
OD 405 nm
Fraction no.
Protein quantification
Non-migrating
Migrating
OD 556 nm
Fraction No.
Sucrose density
Migrating
Non Migrating
Sucrose density (%)
Fraction No.

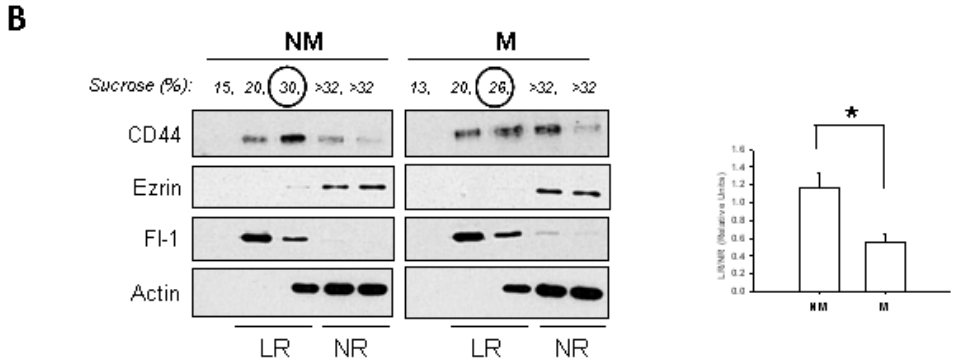
B
NM
M
Sucrose (%):
15, 20, 30, >32, >32
13, 20, 26, >32, >32
CD44
Ezrin
FI-1
Actin
LR
NR
LR
NR
*
NM
M

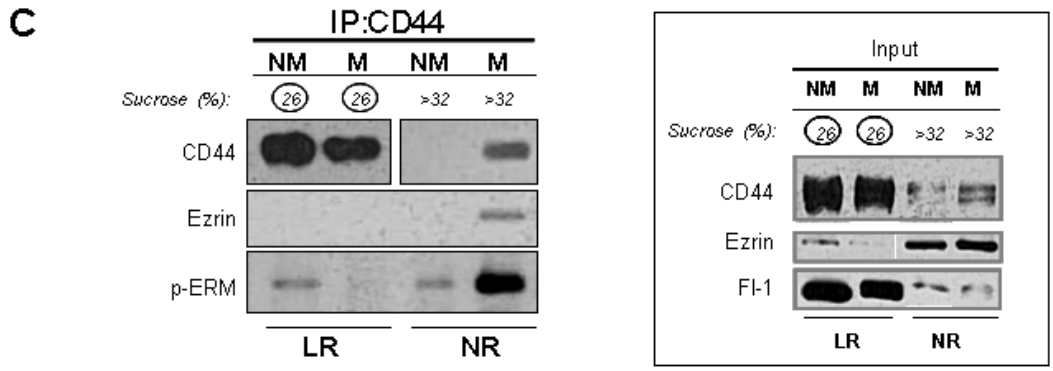
C
IP:CD44
NM
M
NM
M
Sucrose (%):
26
26
>32
>32
CD44
Ezrin
p-ERM
LR
NR
Input
NM
M
NM
M
Sucrose (%):
26
26
>32
>32
CD44
Ezrin
FI-1
LR
NR

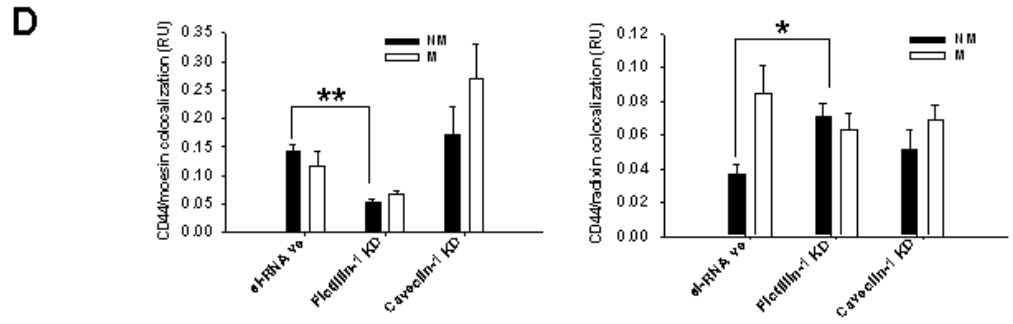
D
CD44/moesin colocalization (RU)
NM
M
**
e-RNA vo
Flotillin-1 KD
Caveolin-1 KD
CD44/radixin colocalization (RU)
NM
M
*
e-RNA vo
Flotillin-1 KD
Caveolin-1 KD

Figure 3

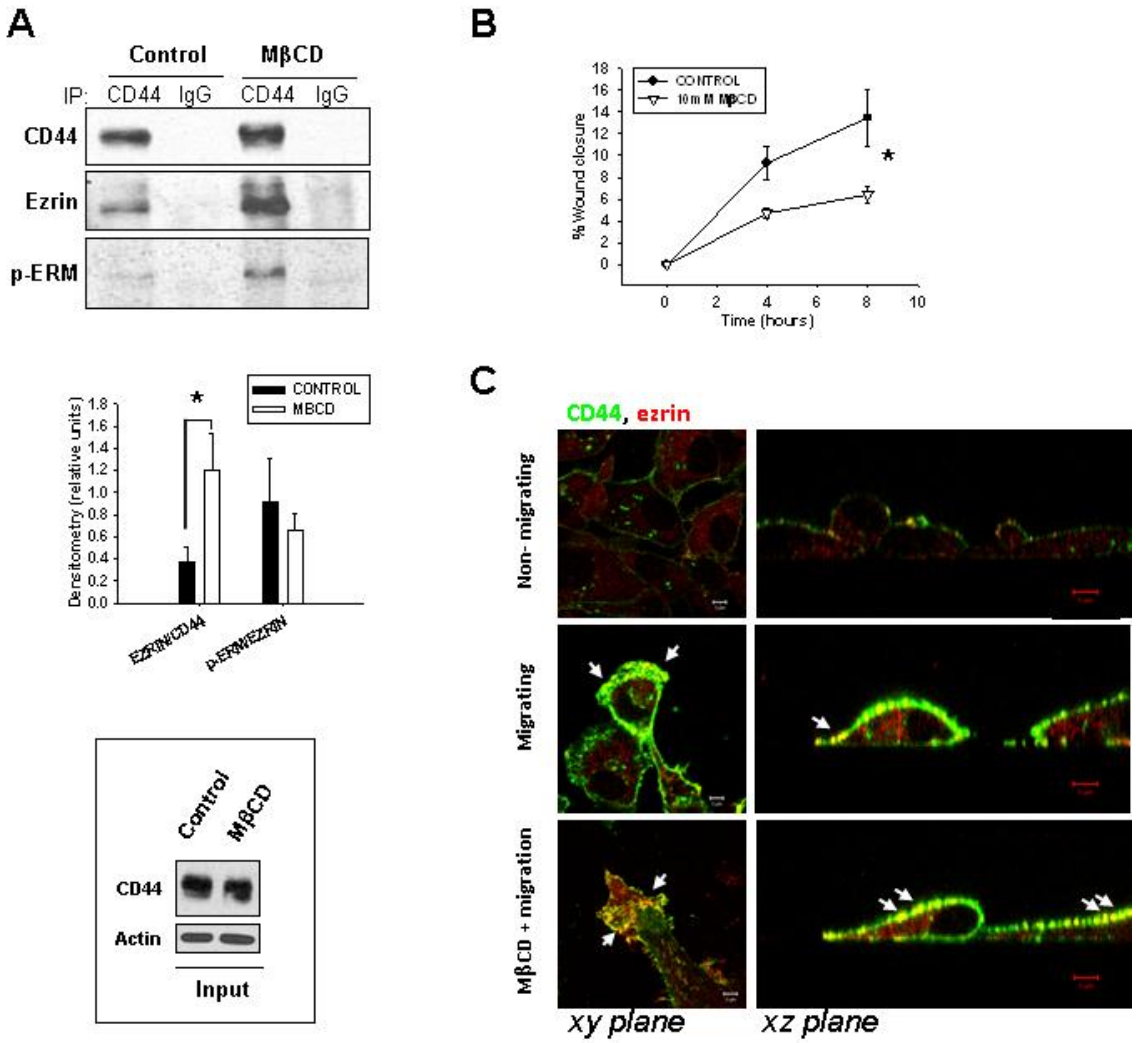
A
Control
MβCD
IP: CD44 IgG CD44 IgG
CD44
Ezrin
p-ERM
CONTROL
MBCD
Densitometry (relative units)
EZRIN/CD44
p-ERM/EZRIN
Control
MβCD
CD44
Actin
Input
B
CONTROL
10 m M MβCD
% Wound closure
Time (hours)
C
CD44, ezrin
Non- migrating
Migrating
MβCD + migration
xy plane
xz plane

Figure 4

A

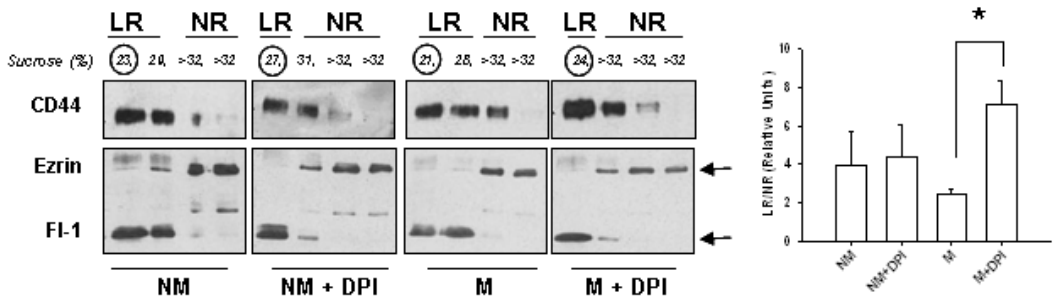
LR
NR
Sucrose (%)
CD44
Ezrin
Fl-1
NM
NM + DPI
M
M + DPI
LR/NR (Relative Units)
NM
NM+DPI
M
M+DPI
*

B

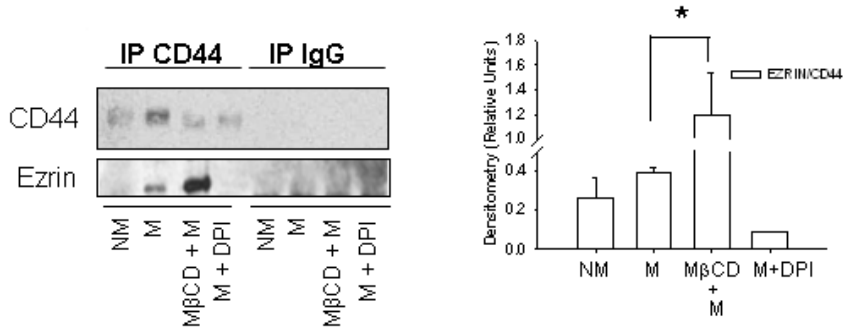
IP CD44
IP IgG
CD44
Ezrin
NM
M
MβCD + M
M + DPI
Densitometry (Relative Units)
EZRIN/CD44
MβCD + M
M+DPI
*

C

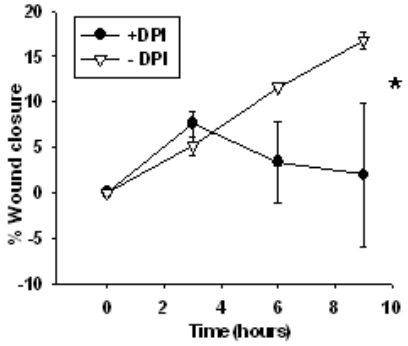
+DPI
- DPI
% Wound closure
Time (hours)
*

Figure 5

A

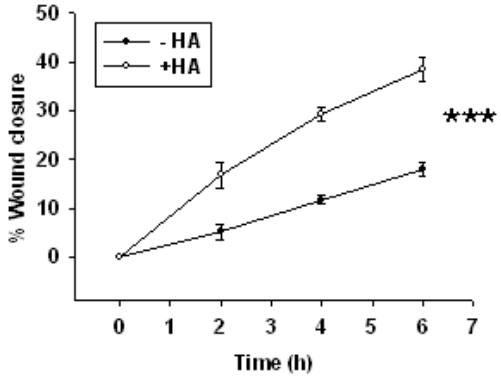
- HA
+HA
% Wound closure
***
Time (h)

B

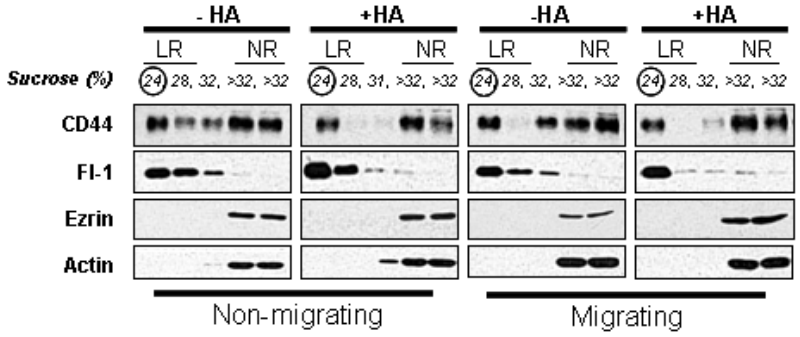
- HA
+HA
-HA
+HA
LR
NR
Sucrose (%)
24 28, 32, >32, >32
24 28, 31, >32, >32
24 28, 32, >32, >32
24 28, 32, >32, >32
CD44
FI-1
Ezrin
Actin
Non-migrating
Migrating

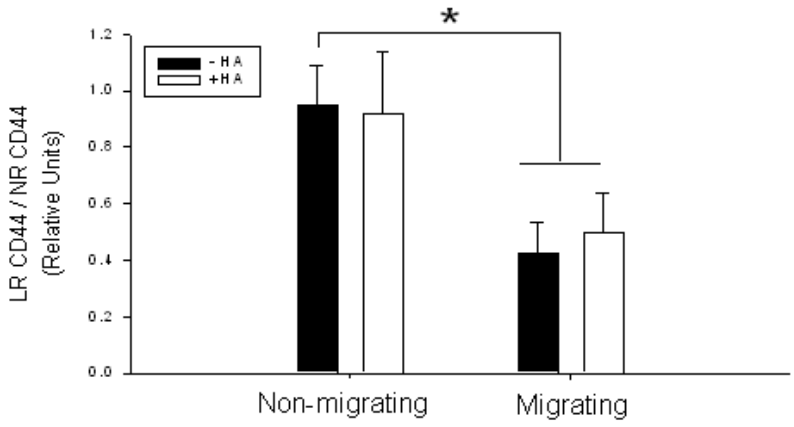
*
- HA
+HA
LR CD44 / NR CD44
(Relative Units)
Non-migrating
Migrating

Figure 6

A

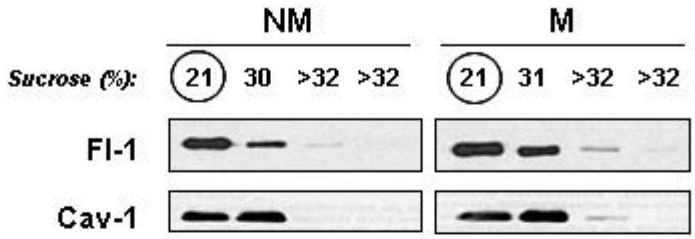
NM
M
Sucrose (%):
21
30
>32
>32
21
31
>32
>32
Fl-1
Cav-1

B

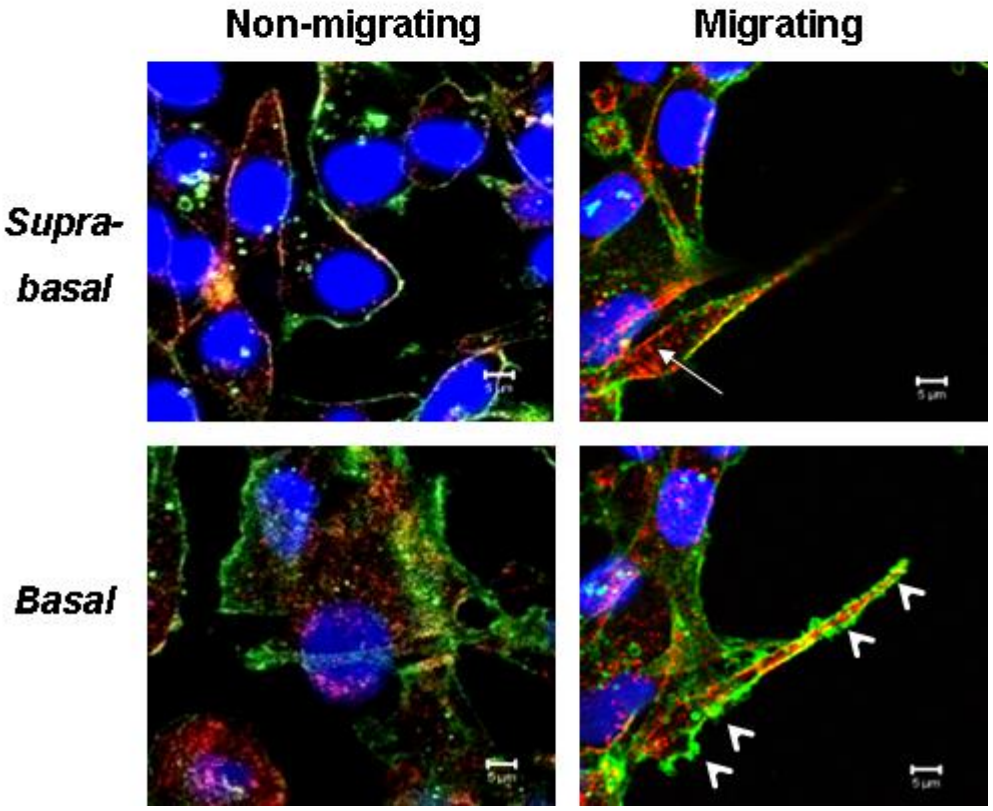
Non-migrating
Migrating
Supra-basal
Basal

Figure 7

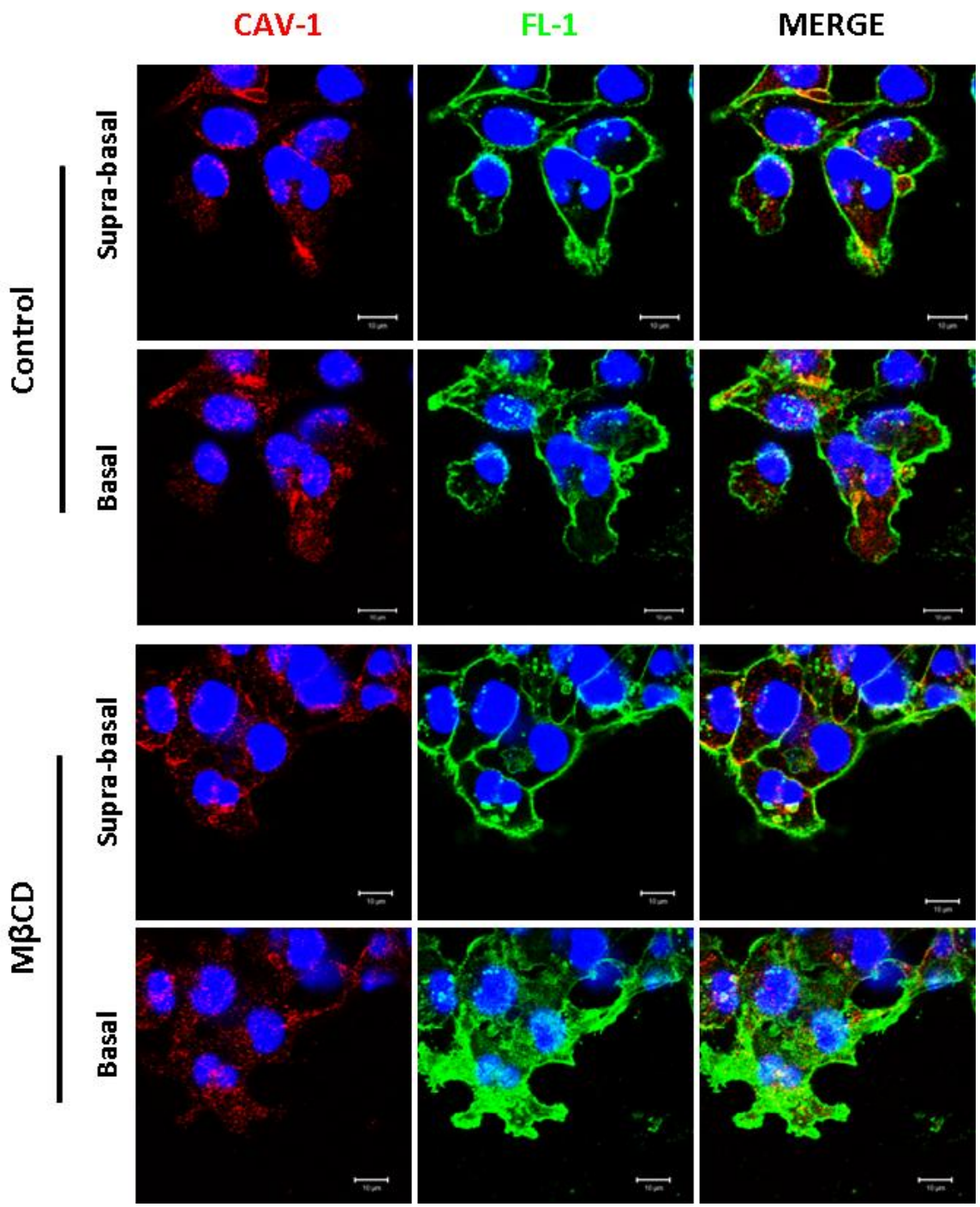
CAV-1
FL-1
MERGE
Control
Supra-basal
Basal
MβCD
Supra-basal
Basal

Figure 8

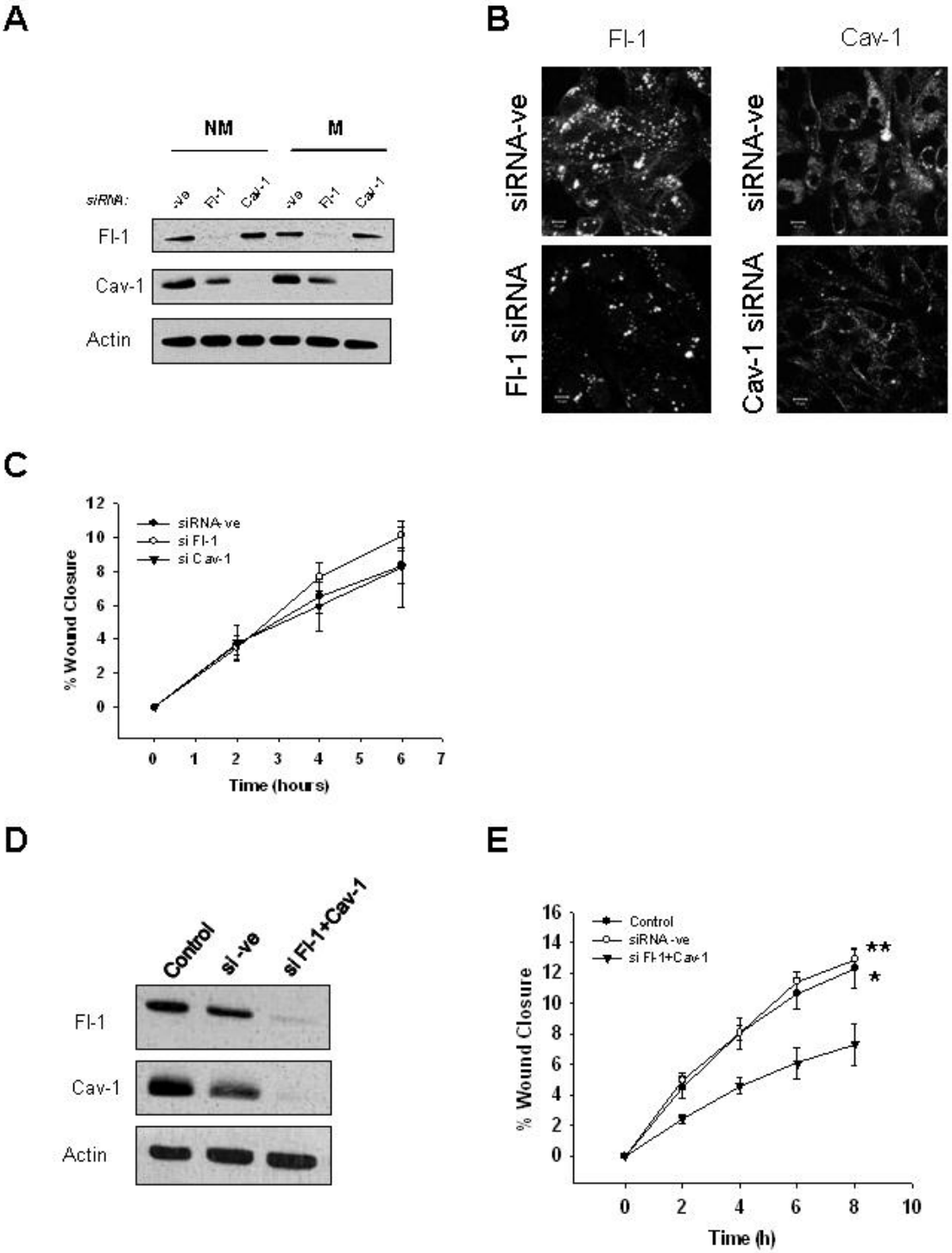
A
NM
M
siRNA:
-ve
Fl-1
Cav-1
-ve
Fl-1
Cav-1
Fl-1
Cav-1
Actin
B
Fl-1
Cav-1
siRNA-ve
siRNA-ve
Fl-1 siRNA
Cav-1 siRNA
C
% Wound Closure
siRNA-ve
si Fl-1
si Cav-1
Time (hours)
D
Control
si -ve
si Fl-1+Cav-1
Fl-1
Cav-1
Actin
E
% Wound Closure
Control
siRNA -ve
si Fl-1+Cav-1
**
*
Time (h)

Figure 9

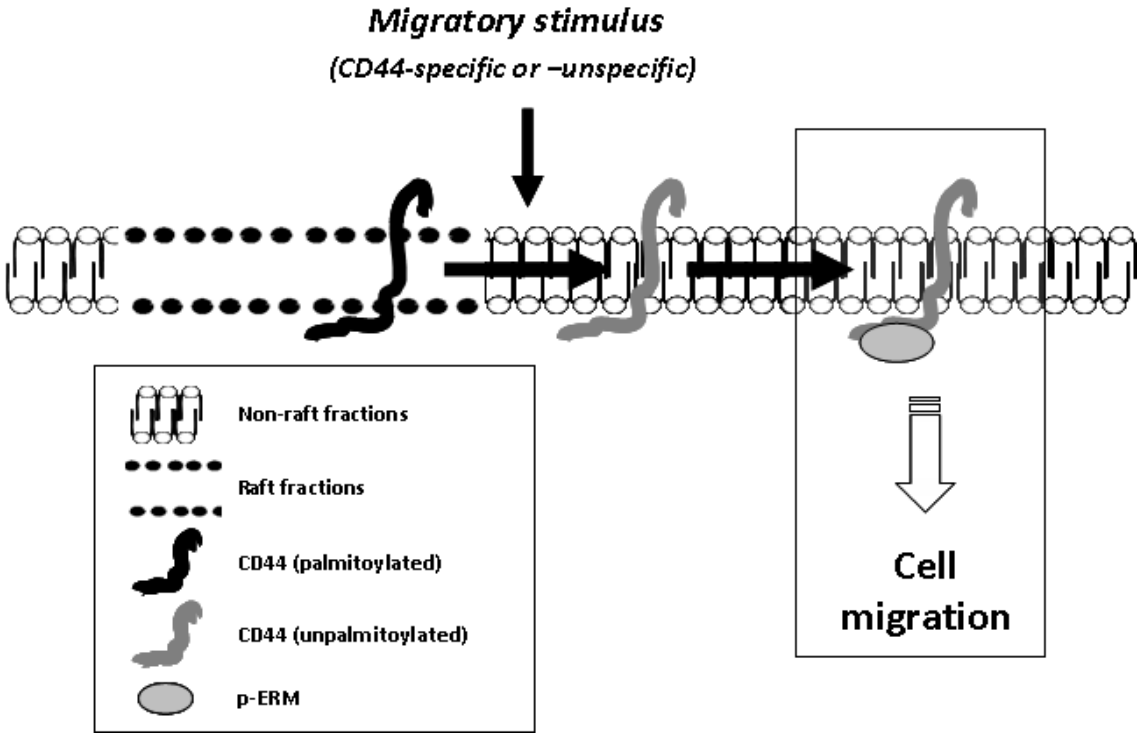
Migratory stimulus
(CD44-specific or –unspecific)
Non-raft fractions
Raft fractions
CD44 (palmitoylated)
CD44 (unpalmitoylated)
p-ERM
Cell migration

Supplementary Figure S1

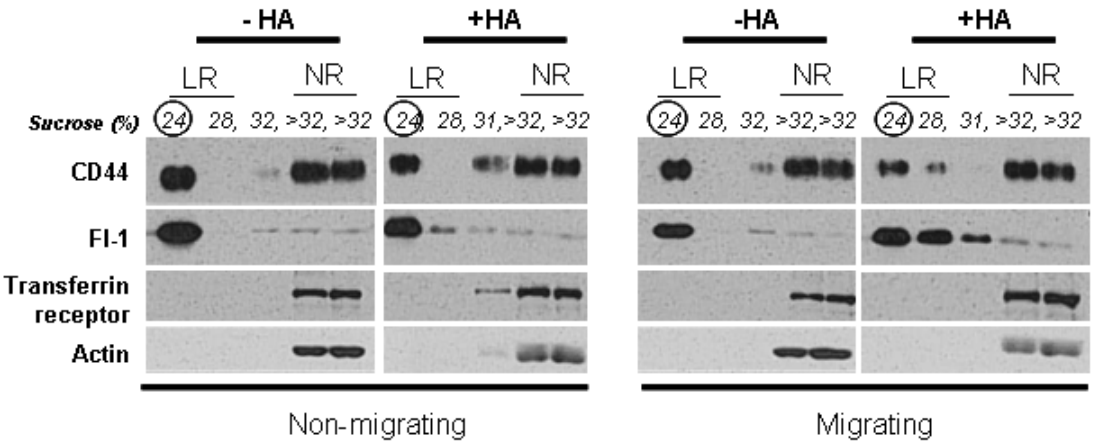

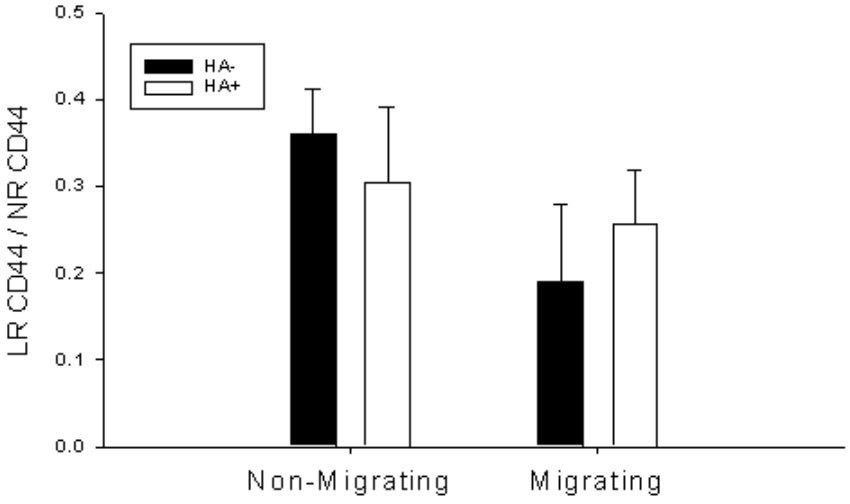

Supplementary Figure S2

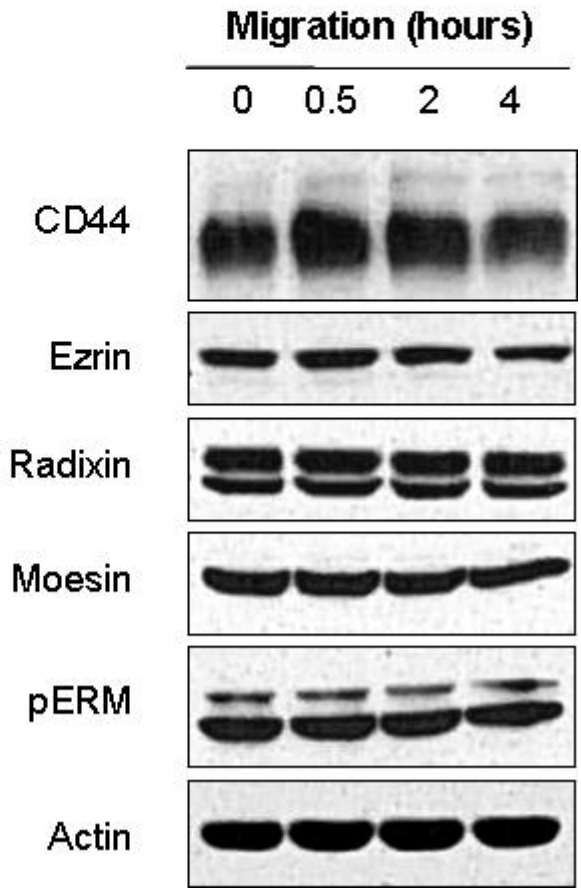

Supplementary Figure S3

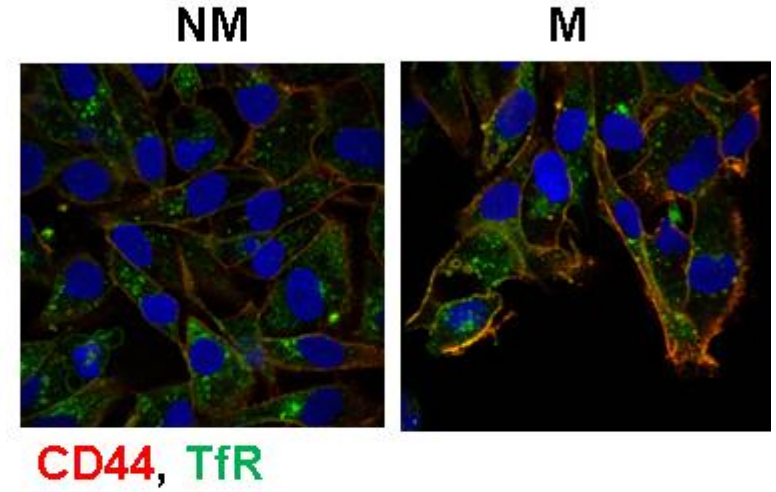

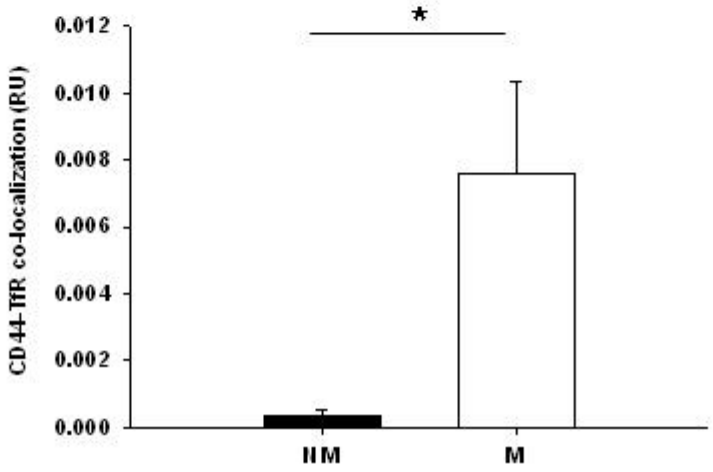

Supplementary Figure S4

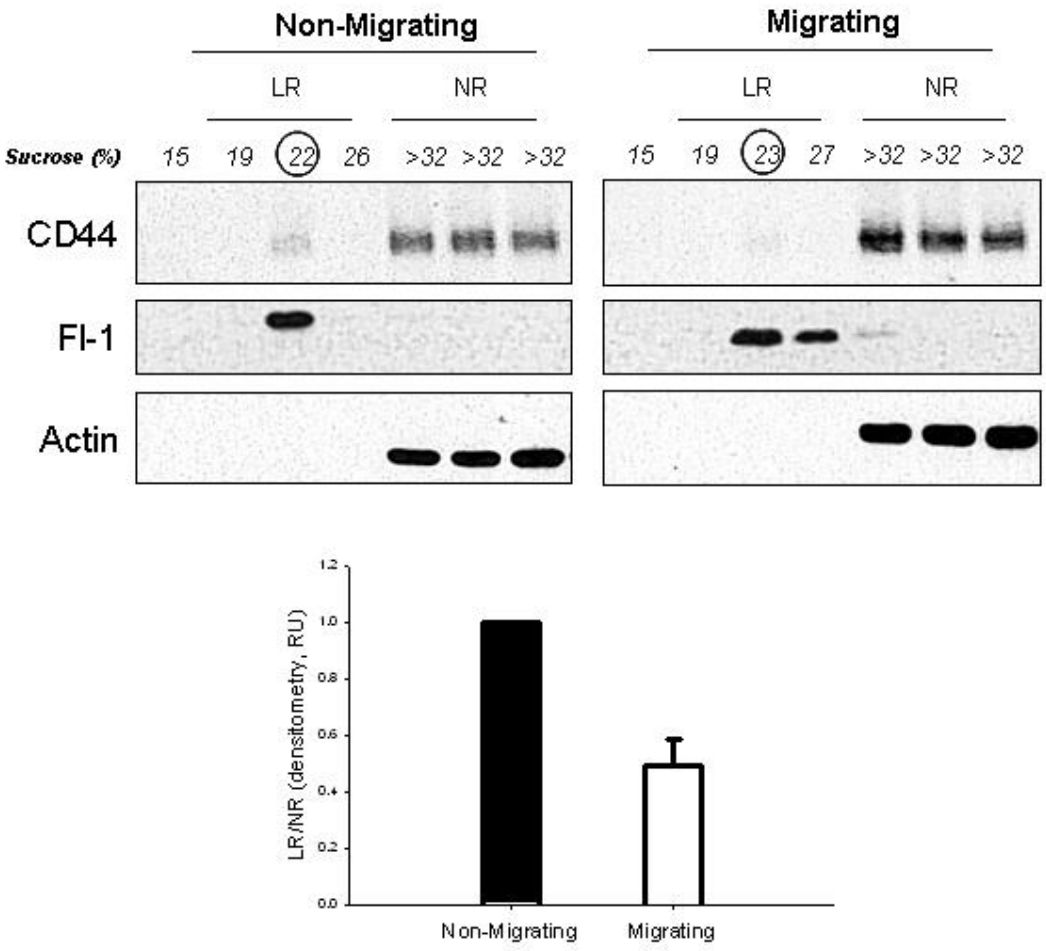

Supplementary Figure S5